Caputo Fractional Differential Equations for Low–risk Individuals of the Tuberculosis Transmission Disease

Nawaz R.[1], Nik Long, N. M. A.[*1], and Shohaimi, S.[2]

[1]*Department of Mathematics and Statistics, Faculty of Science,*
Universiti Putra Malaysia, 43400 Serdang, Selangor, Malaysia
[2]*Department of Biology, Faculty of Science,*
Universiti Putra Malaysia, 43400 Serdang, Selangor, Malaysia

E-mail: nmasri@upm.edu.my
[*]Corresponding author

Abstract

In this article, the Caputo fractional order model with low risk individuals of the tuberculosis is proposed. We investigate a qualitative analysis of the epidemic model via positivity, existence and uniqueness, stability and threshold quantity. Conducting a sensitivity analysis and examining the dynamics of threshold parameters enable the assessment of the efficacy of preventive measures, prediction of future outbreaks, and the formulation of potential strategies for disease control. Numerical computations are executed using the Laplace Adomian decomposition method. The findings imply that the increment of low risk individuals can mitigate the prevalence and impact of tuberculosis on the human population in the respective region.

Keywords: tuberculosis; stability analysis; Laplace Adomian decomposition method.

1   Introduction

Tuberculosis (TB) originates by the Mycobacterium TB bacteria and most commonly affects the lungs. It is treatable and can be prevented. When individuals afflicted with lungs TB engage in activities such as coughing, sneezing, or spitting, they emit TB germs into the surrounding air. Infection occurs due to breathing a small number of these bacterium. TB disease can be transmitted in the following ways: when people with active pulmonary TB cough, sneeze, speak, sing or spit, they emit infectious aerosol droplets ranging in size from 0.5 to 5.0 micrometers. One sneeze can release up to forty thousand droplets. The infectious dosage of TB is extremely low–inhaling less than 10 germs can result in an infection. Therefore, every droplet has the ability to transmit the infection [34, 31]. A significant portion of the world's population has latent TB, which means they have been infected but are not yet sick or contagious. Those carrying TB bacteria have a 5–15% probability of developing the disease in their entire life. Individuals with weak immune systems, including those with HIV, experiencing malnutrition, diabetes, or smoker, have a considerably heightened risk of contacting illness. Inadequate treatment leads to the death of around 45% of individuals without HIV and almost all individuals with HIV who have TB [48].

TB ranks among the world's top ten leading causes of mortality and the second largest infectious killer after COVID–19. According to the World Health Organization (WHO), TB afflicted 10.4 million people, and 1.7 million fatalities, including 0.4 million people living with HIV in 2016. Over 95% of TB fatalities take place in low and middle income countries. In 2016, around one million children were diagnosed with TB, and 0.25 million deaths from TB, which included cases of TB associated with HIV in children. TB is the predominant cause of death in HIV–positive patients, 40% of HIV associated fatalities were due to TB in 2016. The TB death rate declined by 37% from 2000 to 2016, due to a 2% decline in TB incidence, and TB diagnosis and treatment saved an approximately 53 million lives. In 2015, the success rate of treatment for newly diagnosed TB was 83% [48]. In 2022, WHO evaluated that 10.6 million individuals worldwide suffered from TB, and 1.3 million deaths from the TB, including 0.167 million individuals living with HIV. An evaluated 5.8 million men, 3.5 million women, and 1.3 million children were diagnosed with TB [51].

Mathematical models possess essential characteristics that prove invaluable in both controlling and investigating the spread of diseases. Mathematical models addressing numerous disease types are documented in the literature including COVID–19 [3], TB control model [2], TB with exogenous reinfection [20], and rubella disease [12]. Over the past few decades, it is evident that the real–world phenomena can be more accurately represented by utilizing non–integer differential equations, incorporating fractional orders for enhanced precision in various fields such as bio-engineering [32], physics [23], bio-medicine and biology [24], and chemical engineering [40]. It can improve forecast accuracy and memory effect in a variety of dynamical systems and more accurately reflect real–world phenomena. One important aspect of fractional–order models is memory effects, which are the phenomena where the system's current state depends on both its prior history and its current situations. Because TB has a protracted incubation period and can remain latent for years before becoming active, memory effects are especially important [4]. A more realistic description of the disease dynamics is possible with fractional–order models, which incorporate non–integer order derivatives and integrals to account for these memory effects [16].

Kumar et al. [27] studied a new fractional order malaria infectious disease model with vaccines application. Gao et al. [18] investigated the SIRD model for lasa disease in pregnant women by using q–homotopy analysis transform method. Mohandoss et al. [33] analyzed the existence of fractional order SVEIR model of hand feet mouth infectious disease. Atokolo et al. [9] utilized Laplace Adomian decomposition method (LADM) to investigate fractional order Zika virus disease model. Abdulaziz et al. [1] solved fractional order system of differential equation via

homotopy perturbation method.

On the other hand, investigating the TB disease is an important research topic. Waaler et al. [47] made an early contribution to the disease epidemiology by introducing a model for TB infection. Ullah et al. [46] used the product integration (PI) rule to study TB model. Kumar et al. [28] studied the existence and uniqueness of fractional order TB model with two type of derivatives. Rashid et al. [41] studied the fractional order SEIR TB model with immune group by using LADM method. Asres et al. [8] formulated a model to account for inadequate treatment and to evaluate the effect of delayed and rapid transmission of TB infection. Liu et al. [29] developed a TB model to investigate its global stability outcomes. Zhang et al. [50] studied a mathematical model for TB infection that accounted for both hospitalized and non–hospitalized infectious groups.

Fractional order mathematical models based on the fractional operator have been used to study TB transmission dynamics. Introducing fractional order models, such as the Caputo fractional order models, provides new ways to analyze the intricate dynamics of TB transmission. These models more accurately represent TB complex natural history, including issues such as the time lag between infection and community response. Furthermore, the Caputo operator is more easy and convenient as compare to other fractional operators. Its advantageous for providing natural modeling compared to other fractional derivatives, as it assumes that the derivative of a constant is zero. This property aligns well with real–world phenomena like epidemics including COVID–19 [7], tumor [36], malaria [43], and mumps virus [35]. Research has shown that the Caputo model outperforms classical integer–order model by 48% in fitting COVID–19 real data [44]. This demonstrates its superior ability to capture the complex dynamics of disease transmission accurately. The Caputo fractional epidemic models have been rigorously studied for stability, ensuring the existence of unique solutions and their stability using fixed point theorems. This provides a strong theoretical foundation for the models including COVID–19 [37], tumor–immune model [11], and syphilis model [17]. However, one limitation of the Caputo technique compared to other fractional derivatives is the lack of a clear physical or geometrical meaning of the fractional order, even for integer–order derivatives. This can make it challenging to directly relate the fractional order to real–world phenomena. Incorporating hereditary traits and population genetics into Caputo fractional epidemic models is complex and requires further research to fully account for genetic factors affecting disease transmission and susceptibility. The Caputo models still relies on simplifying assumptions like homogeneous mixing of the population. Extending the models to more realistic network–based models could enhance their predictive power like SIR COVID–19 model [6], mass spring model [15], and nipah virus model [13]. Hattaf et al. [22, 21] introduced new mixed fractional derivative and Fractal fractional derivative definitions in the sense of Caputo. Owolabi and Pindza [38] worked on the Caputo type fractional order model of TB with constant control measures. Many other researchers worked on TB models in different way, refer for more details [42, 10].

In this paper, we extend the integer order epidemiological model of Liu & Wang [30] which integrates interventions via Caputo fractional derivative. The Caputo derivative used in this study is a special case of the new Hattaf mixed fractional derivative. The proposed model having epidemiological relevance which provides the comparison between traditional compartmental model with complex dynamic of TB transmission via LADM numerical method. In addition, compared to other approaches, the Laplace–Adomian algorithm has a stronger convergence rate and is straightforward and easy to use. It can be seen that, in spite of these benefits, its stability is inferior to that of other numerical methods [49]. The uniqueness of this paper includes: fractional derivative, multi component structure, data integration, sensitivity analysis, and novel mathematical method. These innovations collectively contribute to the novelty of the TB model, making it a more comprehensive and accurate tool for understanding and controlling the disease. The entire population in the model, denoted as $N(z)$, is segmented into eight distinct categories: the sus-

ceptible class $S(z)$, the early latent class $E_e(z)$, the later latent class $E_l(z)$, the infected TB class $I(z)$, the treatment TB class $T(z)$, the active TB with interrupted treatment class $G(z)$, the low–risk individuals class $L_r(z)$, and the recovered class $R(z)$. The total population is expressed as $N(z) = S(z) + E_e(z) + E_l(z) + I(z) + T(z) + G(z) + L_r(z) + R(z)$. The fractional order for $SE_eE_lITGL_rR$ is formulated as follows:

$$
\begin{cases}
{}^{C}D^{\vartheta}S = \Lambda + \theta R - \beta SI - \mu S, \\
{}^{C}D^{\vartheta}E_e = \beta SI + (1-q)\eta G - (m + \mu + k)E_e, \\
{}^{C}D^{\vartheta}E_l = (1-p)kE_e + q\eta G - (\mu + \omega)E_l, \\
{}^{C}D^{\vartheta}I = pkE_e + \omega E_l - (r + \mu + d_1)I + \sigma\rho T, \\
{}^{C}D^{\vartheta}T = rI - (\mu + d_2 + \gamma + \xi + \sigma)T, \\
{}^{C}D^{\vartheta}G = \gamma T - (\mu + d_3 + \eta)G, \\
{}^{C}D^{\vartheta}L_r = (1-\rho)\sigma T + mE_e - \mu L_r, \\
{}^{C}D^{\vartheta}R = \xi T - (\mu + \theta)R.
\end{cases}
\tag{1}
$$

In Model (1), $\vartheta \in (0, 1]$ denotes the fractional order, Λ represents the rate of introduction of the susceptible population, and β indicates the rate of transmission coefficient from the susceptible S to the infected I. Furthermore, μ signifies the natural death rate, whereas d_1, d_2, and d_3 indicate the disease–induced fatality rates in classes I, T, and G, respectively. ω represents the reactivation rate of the long–term latent population. p shows the proportion of people in the early latent stage with rapid TB progression. The parameter q indicates the percentage of self–cured persons in class G who move to class E_l. ξ denotes the recovery rate of treated active TB cases. The rate of treatment interruption in class T is illustrated by γ. η denotes the rate at which persons in class G self–cure due to the immune system, whereas r represents the rate of treatment for untreated active TB cases and k symbolizes the reactivation rate of the early latent stage. The treatment failure probability is represented by ρ, the treatment rate by σ, and the progression rate from E_e to L_r by m. Finally, θ denotes the proportion of recovered people that become sensitive again and re–enter the susceptible class.
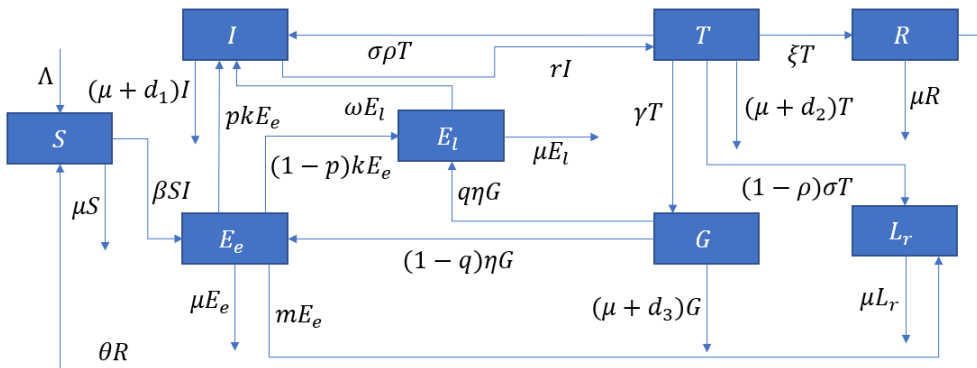

Figure 1: Schematic diagram of TB Model (2).

The schematic diagram of the dynamical Model (1) is depicted in Figure 1. The outward arrows symbolize the terms exiting the compartments, whereas inward arrows signify the terms entering the compartments. Considering the total population $N(z)$, it is reasonable to assume that for $z \geq 0$, all variables are greater than or equal to zero.

For simplicity Model (1) can be written as,

$$
\begin{cases}
{}^{C}D^{\vartheta}S = \Lambda + \theta R - \beta SI - \mu S, \\
{}^{C}D^{\vartheta}E_e = \beta SI + k_1 G - k_2 E_e, \\
{}^{C}D^{\vartheta}E_l = k_3 E_e + q\eta G - k_4 E_l, \\
{}^{C}D^{\vartheta}I = pk E_e + \omega E_l - k_5 I + \sigma \rho T, \\
{}^{C}D^{\vartheta}T = rI - k_6 T, \\
{}^{C}D^{\vartheta}G = \gamma T - k_7 G, \\
{}^{C}D^{\vartheta}L_r = k_8 T + m E_e - \mu L_r, \\
{}^{C}D^{\vartheta}R = \xi T - k_9 R, \\
S \geq 0, \quad E_e \geq 0, \quad E_l \geq 0, \quad I \geq 0, \\
T \geq 0, \quad G \geq 0, \quad L_r \geq 0, \quad R \geq 0,
\end{cases}
\tag{2}
$$

where, $k_1 = (1-q)\eta$, $k_2 = m + \mu + k$, $k_3 = (1-p)k$, $k_4 = \mu + \omega$, $k_5 = r + \mu + d_1 + \sigma$, $k_6 = \mu + d_2 + \gamma + \xi + \sigma$, $k_7 = \mu + d_3 + \eta$, $k_8 = (1-\rho)\sigma$, $k_9 = \mu + \theta$. Further details regarding parameters are outlined in the Table 1.

Table 1: Parameters description of the TB model.

Parameter	Description
Λ	recruitment rate
θ	fraction of recovered individuals being suspected
β	rate of transmission from S to I
μ	natural fatality rate
q	rate of self cured person from G enter into E_l
η	rate of self cured persons in G due to immune system
m	progression rate from E_e to L_r
k	reactivation rate of the early latent persons
p	latent persons fast TB progression rate
ω	reactivation rate of long term latent individuals
r	rate of treatment for untreated active TB cases
d_1	disease induced fatality rate in I
σ	treatment rate
ρ	treatment failure probability
d_2	TB induced fatality rate in T
γ	treatment rate interruption in class T
ξ	recovery rate
d_3	disease induced fatality rate in G
ϑ	fractional order

In this manuscript, sections are arranged as follows: Section 1 details the proposed dynamical system for investigating TB disease dynamics. Section 2 offers some necessary definitions, lemmas and theorems. Section 3 discusses the existence and uniqueness of solutions. The calculation of the basic reproduction number, disease–free and endemic equilibrium points, and stability analysis are presented in Section 4. Section 5 covers the sensitivity analysis. The construction of general solution of the proposed model by LADM and some numerical results are displayed in Section 6. Finally, Section 7 delves into the conclusions.

2   Preliminaries

Definition 2.1. [25] *The fractional ϑ-order integral of a function* $\mathrm{x} : R^+ \to R$ *is defined as,*

$$I^\vartheta \mathrm{x}(z) = \frac{1}{\Gamma(\vartheta)} \int_0^z (z-s)^{\vartheta-1} \mathrm{x}(s) ds.$$

$\Gamma(.)$ *is gamma function and the integral exists.*

Definition 2.2. [25] *The fractional ϑ order Caputo type derivative of a function* $\mathrm{x} \in C^{(\rho)}\big((0,\infty), \mathsf{R}\big)$ *is defined as,*

$$^C D^\vartheta \mathrm{x}(z) = \frac{1}{\Gamma(\rho - \vartheta)} \int_0^z (z-s)^{\rho-\vartheta-1} \mathrm{x}^\rho(s) ds,$$

where $\rho = [\vartheta] + 1$ and $[\vartheta]$ is integer part of $\vartheta \in R^+$.

Corollary 2.1. [19] *Let $f(z) \in C[c,d]$, $D^\vartheta f(z) \in C[c,d]$, and $\vartheta \in (0,1]$. For all $z \in (c,d)$ then, if $D^\vartheta f(z) \geq 0$ then $f(z)$ is non–decreasing, and if $D^\vartheta f(z) \leq 0$ then $f(z)$ is non–increasing.*

Definition 2.3. [39] *Laplace transformation of the Caputo type derivative is defined as,*

$$\mathsf{L}[^C D^\vartheta f(z)] = s^\vartheta F(s) - \sum_{j=0}^{n-1} s^{\vartheta-j-1} f^j(0), \quad n-1 < \vartheta < n, \quad n \in N.$$

3   Main Results

3.1   Existence and uniqueness of model (2)

Model (2) can be rewritten as,

$$\begin{cases} {}^C D^\vartheta S(z) = \mathcal{A}_1(z, S(z)) = \Lambda + \theta R - \beta SI - \mu S, \\ {}^C D^\vartheta E_e(z) = \mathcal{A}_2(z, E_e(z)) = \beta SI + k_1 G - k_2 E_e, \\ {}^C D^\vartheta E_l(z) = \mathcal{A}_3(z, E_l(z)) = k_3 E_e + q\eta G - k_4 E_l, \\ {}^C D^\vartheta I(z) = \mathcal{A}_4(z, I(z)) = pk E_e + \omega E_l - k_5 I + \sigma\rho T, \\ {}^C D^\vartheta T(z) = \mathcal{A}_5(z, T(z)) = rI - k_6 T, \\ {}^C D^\vartheta G(z) = \mathcal{A}_6(z, G(z)) = \gamma T - k_7 G, \\ {}^C D^\vartheta L_r(z) = \mathcal{A}_7(z, L_r(z)) = k_8 T + m E_e - \mu L_r, \\ {}^C D^\vartheta R(z) = \mathcal{A}_8(z, R(z)) = \xi T - k_9 R. \end{cases} \quad (3)$$

To simplify, we write Model (3) in vector form as,

$$\begin{cases} {}^C D^\vartheta \mathcal{U}(z) = \mathcal{Z}(z, \mathcal{U}(z)), \\ \quad \mathcal{U}(0) = \mathcal{U}_0 \geq 0, \quad 0 \leq z \leq T < \infty, \quad 0 < \vartheta \leq 1, \end{cases} \quad (4)$$

where $\mathcal{U}(z)$, $\mathcal{U}(0)$ represents vectors containing the state variables and their initial values respectively, and $\mathcal{Z} : [0, T] \times R^8 \to R$ is a continuous vector function, i.e.,

$$\begin{cases} \quad \mathcal{U}(z) = (S, E_e, E_l, I, T, G, L_r, R)^T, \\ \quad \mathcal{U}(0) = (S_0, E_{e_0}, E_{l_0}, I_0, T_0, G_0, L_{r_0}, R_0)^T, \\ \mathcal{Z}(z, \mathcal{U}(z)) = \big[\mathcal{A}_i(S, E_e, E_l, I, T, G, L_r, R)\big]^T, \quad i = 1, \dots, 8. \end{cases}$$

Integrate both sides of (4), from 0 to z, gives,

$$\mathcal{U}(z) - \mathcal{U}(0) = \frac{1}{\Gamma(\vartheta)} \int_0^z \mathcal{Z}(y, \mathcal{U}(y))(z-y)^{\vartheta-1} dy, \tag{5}$$

for each population, (5) can be expressed as,

$$\begin{cases} S(z) - S(0) = \frac{1}{\Gamma(\vartheta)} \int_0^z (z-y)^{\vartheta-1} \Big[\mathcal{A}_1(y, S(y)) \Big] dy, \\ E_e(z) - E_e(0) = \frac{1}{\Gamma(\vartheta)} \int_0^z (z-y)^{\vartheta-1} \Big[\mathcal{A}_2(y, E_e(y)) \Big] dy, \\ E_l(z) - E_l(0) = \frac{1}{\Gamma(\vartheta)} \int_0^z (z-y)^{\vartheta-1} \Big[\mathcal{A}_3(y, E_l(y)) \Big] dy, \\ I(z) - I(0) = \frac{1}{\Gamma(\vartheta)} \int_0^z (z-y)^{\vartheta-1} \Big[\mathcal{A}_4(y, I(y)) \Big] dy, \\ T(z) - T(0) = \frac{1}{\Gamma(\vartheta)} \int_0^z (z-y)^{\vartheta-1} \Big[\mathcal{A}_5(y, T(y)) \Big] dy, \\ G(z) - G(0) = \frac{1}{\Gamma(\vartheta)} \int_0^z (z-y)^{\vartheta-1} \Big[\mathcal{A}_6(y, G(y)) \Big] dy, \\ L_r(z) - L_r(0) = \frac{1}{\Gamma(\vartheta)} \int_0^z (z-y)^{\vartheta-1} \Big[\mathcal{A}_7(y, L_r(y)) \Big] dy, \\ R(z) - R(0) = \frac{1}{\Gamma(\vartheta)} \int_0^z (z-y)^{\vartheta-1} \Big[\mathcal{A}_8(y, R(y)) \Big] dy. \end{cases} \tag{6}$$

Theorem 3.1. *All kernels,*

$$\mathcal{A}_i, \quad i = 1, \dots, 8,$$

satisfy the Lipschitz condition and they are contraction if the following inequality holds,

$$0 \leq \gamma_i < 1, \quad i = 1, \dots, 8.$$

Proof. Let S and S_1 be two functions, then we have

$$\|\mathcal{A}_1(z, S(z)) - \mathcal{A}_1(z, S_1(z))\| = \| -\beta\{S(z) - S_1(z)\}I(z) - \mu\{S(z) - S_1(z)\}\|.$$

Taking $\gamma_1 = \beta d + \mu$, $\|I(z)\| \leq d$, by triangular inequality, we have

$$\begin{aligned} \|\mathcal{A}_1(z, S(z)) - \mathcal{A}_1(z, S_1(z))\| &\leq \|\beta(S(z) - S_1(z))I(z)\| + \|\mu(S(z) - S_1(z))\| \\ &\leq (\beta\|I(z)\| + \mu)\|S(z) - S_1(z)\| \\ &\leq (\beta d + \mu)\|S(z) - S_1(z)\| \\ &\leq \gamma_1\|S(z) - S_1(z)\|. \end{aligned}$$

Similarly,

$$\begin{cases} \|\mathcal{A}_2(z, E_e(z)) - \mathcal{A}_2(z, E_{e_1}(z))\| \leq \gamma_2\|E_e(z) - E_{e_1}(z)\|, \\ \|\mathcal{A}_3(z, E_l(z)) - \mathcal{A}_3(z, E_{l_1}(z))\| \leq \gamma_3\|E_l(z) - E_{l_1}(z)\|, \\ \|\mathcal{A}_4(z, I(z)) - \mathcal{A}_4(z, I_1(z))\| \leq \gamma_4\|I(z) - I_1(z)\|, \\ \|\mathcal{A}_5(z, T(z)) - \mathcal{A}_5(z, T_1(z))\| \leq \gamma_5\|T(z) - T_1(z)\|, \\ \|\mathcal{A}_6(z, G(z)) - \mathcal{A}_6(z, G_1(z))\| \leq \gamma_6\|G(z) - G_1(z)\|, \\ \|\mathcal{A}_7(z, L_r(z)) - \mathcal{A}_7(z, L_{r_1}(z))\| \leq \gamma_7\|L_r(z) - L_{r_1}(z)\|, \\ \|\mathcal{A}_8(z, R(z)) - \mathcal{A}_8(z, R_1(z))\| \leq \gamma_8\|R(z) - R_1(z)\|, \end{cases}$$

where $\gamma_1 = \beta d + \mu$, $\gamma_2 = k_2$, $\gamma_3 = k_4$, $\gamma_4 = k_5$, $\gamma_5 = k_6$, $\gamma_6 = k_7$, $\gamma_7 = \mu$, $\gamma_8 = k_9$. Hence, all $\mathcal{A}_i$ satisfy the Lipschitz condition, and they are also contraction if $0 \leq \gamma_i < 1$, where $i = 2, \dots, 8$.

From (6), the recursive formula for S, E_e, E_l, I, T, G, L_r, R are

$$
\begin{cases}
S_n(z) = \frac{1}{\Gamma(\vartheta)} \int_0^z (z-y)^{\vartheta-1} \Big[\mathcal{A}_1(y, S_{n-1}(y)) \Big] dy, \\
E_{e_n}(z) = \frac{1}{\Gamma(\vartheta)} \int_0^z (z-y)^{\vartheta-1} \Big[\mathcal{A}_2(y, E_{e_{n-1}}(y)) \Big] dy, \\
E_{l_n}(z) = \frac{1}{\Gamma(\vartheta)} \int_0^z (z-y)^{\vartheta-1} \Big[\mathcal{A}_3(y, E_{l_{n-1}}(y)) \Big] dy, \\
I_n(z) = \frac{1}{\Gamma(\vartheta)} \int_0^z (z-y)^{\vartheta-1} \Big[\mathcal{A}_4(y, I_{n-1}(y)) \Big] dy, \\
T_n(z) = \frac{1}{\Gamma(\vartheta)} \int_0^z (z-y)^{\vartheta-1} \Big[\mathcal{A}_5(y, T_{n-1}(y)) \Big] dy, \\
G_n(z) = \frac{1}{\Gamma(\vartheta)} \int_0^z (z-y)^{\vartheta-1} \Big[\mathcal{A}_6(y, G_{n-1}(y)) \Big] dy, \\
L_{r_n}(z) = \frac{1}{\Gamma(\vartheta)} \int_0^z (z-y)^{\vartheta-1} \Big[\mathcal{A}_7(y, L_{r_{n-1}}(y)) \Big] dy, \\
R_n(z) = \frac{1}{\Gamma(\vartheta)} \int_0^z (z-y)^{\vartheta-1} \Big[\mathcal{A}_8(y, R_{n-1}(y)) \Big] dy,
\end{cases}
$$

with initial conditions;

$$
\begin{aligned}
S_0(z) = S(0), \quad & E_{e_0}(z) = E_e(0), \quad E_{l_0}(z) = E_l(0), \quad I_0(z) = I(0), \\
T_0(z) = T(0), \quad & G_0(z) = G(0), \quad L_{r_0}(z) = L_r(0), \quad R_0(z) = R(0).
\end{aligned}
$$

Now, taking the differences between the successive terms yields,

$$
\begin{cases}
\varphi_{1n}(z) = S_n(z) - S_{n-1}(z) = \frac{1}{\Gamma(\vartheta)} \int_0^z (z-y)^{\vartheta-1} \Big[\mathcal{A}_1(y, S_{n-1}(y)) - \mathcal{A}_1(y, S_{n-2}(y)) \Big] dy, \\
\varphi_{2n}(z) = E_{e_n}(z) - E_{e_{n-1}}(z) = \frac{1}{\Gamma(\vartheta)} \int_0^z (z-y)^{\vartheta-1} \Big[\mathcal{A}_2(y, E_{e_{n-1}}(y)) - \mathcal{A}_2(y, E_{e_{n-2}}(y)) \Big] dy, \\
\varphi_{3n}(z) = E_{l_n}(z) - E_{l_{n-1}}(z) = \frac{1}{\Gamma(\vartheta)} \int_0^z (z-y)^{\vartheta-1} \Big[\mathcal{A}_3(y, E_{l_{n-1}}(y)) - \mathcal{A}_3(y, E_{l_{n-2}}(y)) \Big] dy, \\
\varphi_{4n}(z) = I_n(z) - I_{n-1}(z) = \frac{1}{\Gamma(\vartheta)} \int_0^z (z-y)^{\vartheta-1} \Big[\mathcal{A}_4(y, I_{n-1}(y)) - \mathcal{A}_4(y, I_{n-2}(y)) \Big] dy, \\
\varphi_{5n}(z) = T_n(z) - T_{n-1}(z) = \frac{1}{\Gamma(\vartheta)} \int_0^z (z-y)^{\vartheta-1} \Big[\mathcal{A}_5(y, T_{n-1}(y)) - \mathcal{A}_5(y, T_{n-2}(y)) \Big] dy, \\
\varphi_{6n}(z) = G_n(z) - G_{n-1}(z) = \frac{1}{\Gamma(\vartheta)} \int_0^z (z-y)^{\vartheta-1} \Big[\mathcal{A}_6(y, G_{n-1}(y)) - \mathcal{A}_6(y, G_{n-2}(y)) \Big] dy, \\
\varphi_{7n}(z) = L_{r_n}(z) - L_{r_{n-1}}(z) = \frac{1}{\Gamma(\vartheta)} \int_0^z (z-y)^{\vartheta-1} \Big[\mathcal{A}_7(y, L_{r_{n-1}}(y)) - \mathcal{A}_7(y, L_{r_{n-2}}(y)) \Big] dy, \\
\varphi_{8n}(z) = R_n(z) - R_{n-1}(z) = \frac{1}{\Gamma(\vartheta)} \int_0^z (z-y)^{\vartheta-1} \Big[\mathcal{A}_8(y, R_{n-1}(y)) - \mathcal{A}_8(y, R_{n-2}(y)) \Big] dy.
\end{cases}
\tag{7}
$$

Applying the norm to both sides of (7), we obtain

$$
\|\varphi_{1n}(z)\| \leq \frac{1}{\Gamma(\vartheta)} \int_0^z \|(z-y)^{\vartheta-1}[\mathcal{A}_1(y, S_{n-1}(y)) - \mathcal{A}_1(y, S_{n-2}(y))]\| dy.
$$

As the kernel fulfills the Lipschitz condition, we have

$$
\|\varphi_{1n}(z)\| \leq \frac{\gamma_1}{\Gamma(\vartheta)} \int_0^z \|\varphi_{1(n-1)}(y)\| dy,
\tag{8}
$$

where γ_1 is the Lipschitz constant.

Similarly, we obtain

$$
\begin{cases}
\|\varphi_{2n}(z)\| \leq \frac{\gamma_2}{\Gamma(\vartheta)} \int_0^z \|\varphi_{2(n-1)}(y)\| dy, \\
\|\varphi_{3n}(z)\| \leq \frac{\gamma_3}{\Gamma(\vartheta)} \int_0^z \|\varphi_{3(n-1)}(y)\| dy, \\
\|\varphi_{4n}(z)\| \leq \frac{\gamma_4}{\Gamma(\vartheta)} \int_0^z \|\varphi_{4(n-1)}(y)\| dy, \\
\|\varphi_{5n}(z)\| \leq \frac{\gamma_5}{\Gamma(\vartheta)} \int_0^z \|\varphi_{5(n-1)}(y)\| dy, \\
\|\varphi_{6n}(z)\| \leq \frac{\gamma_6}{\Gamma(\vartheta)} \int_0^z \|\varphi_{6(n-1)}(y)\| dy, \\
\|\varphi_{7n}(z)\| \leq \frac{\gamma_7}{\Gamma(\vartheta)} \int_0^z \|\varphi_{7(n-1)}(y)\| dy, \\
\|\varphi_{8n}(z)\| \leq \frac{\gamma_8}{\Gamma(\vartheta)} \int_0^z \|\varphi_{8(n-1)}(y)\| dy.
\end{cases}
\tag{9}
$$

Then we can write as,

$$
\begin{cases}
S_n(z) = \sum_{i=1}^n \varphi_{1i}(z), \quad E_{e_n}(z) = \sum_{i=1}^n \varphi_{2i}(z), \quad E_{l_n}(z) = \sum_{i=1}^n \varphi_{3i}(z), \quad I_n(z) = \sum_{i=1}^n \varphi_{4i}(z), \\
T_n(z) = \sum_{i=1}^n \varphi_{5i}(z), \quad G_n(z) = \sum_{i=1}^n \varphi_{6i}(z), \quad L_{r_n}(z) = \sum_{i=1}^n \varphi_{7i}(z), \quad R_n(z) = \sum_{i=1}^n \varphi_{8i}(z).
\end{cases}
$$

□

In the following theorem, we prove the existence of a solution.

Theorem 3.2. *The solution to the epidemiological Model* (2) *exists for finite time z_0, if,*

$$
\frac{\gamma_i}{\Gamma(\vartheta)} z_0 < 1, \ \forall \ i = 1, \ldots, 8.
$$

Proof. By using (8), (9), and recursive principle [5], we obtain

$$
\begin{cases}
\|\varphi_{1n}(z)\| \leq \|S(0)\| \left[\frac{\gamma_1}{\Gamma(\vartheta)} z \right]^n, \\
\|\varphi_{2n}(z)\| \leq \|E_e(0)\| \left[\frac{\gamma_2}{\Gamma(\vartheta)} z \right]^n, \\
\|\varphi_{3n}(z)\| \leq \|E_l(0)\| \left[\frac{\gamma_3}{\Gamma(\vartheta)} z \right]^n, \\
\|\varphi_{4n}(z)\| \leq \|I(0)\| \left[\frac{\gamma_4}{\Gamma(\vartheta)} z \right]^n, \\
\|\varphi_{5n}(z)\| \leq \|T(0)\| \left[\frac{\gamma_5}{\Gamma(\vartheta)} z \right]^n, \\
\|\varphi_{6n}(z)\| \leq \|G(0)\| \left[\frac{\gamma_6}{\Gamma(\vartheta)} z \right]^n, \\
\|\varphi_{7n}(z)\| \leq \|L_r(0)\| \left[\frac{\gamma_7}{\Gamma(\vartheta)} z \right]^n, \\
\|\varphi_{8n}(z)\| \leq \|R(0)\| \left[\frac{\gamma_8}{\Gamma(\vartheta)} z \right]^n.
\end{cases}
$$

Hence, Model (2) has at least one solution and are continuous.

Now, we prove that the functions $S_n(z)$, $E_{e_n}(z)$, $E_{l_n}(z)$, $I_n(z)$, $T_n(z)$, $G_n(z)$, $L_{r_n}(z)$ and $R_n(z)$ converges to the solutions of Model (2). Let $\mathcal{B}_{1n}(z)$, $\mathcal{B}_{2n}(z)$, $\mathcal{B}_{3n}(z)$, $\mathcal{B}_{4n}(z)$, $\mathcal{B}_{5n}(z)$, $\mathcal{B}_{6n}(z)$, $\mathcal{B}_{7n}(z)$

and $\mathcal{B}_{8n}(z)$ are remainders terms after n iterations, then,

$$
\begin{cases}
S(z) - S(0) = S_n(z) - \mathcal{B}_{1n}(z), \\
E_e(z) - E_e(0) = E_{e_n}(z) - \mathcal{B}_{2n}(z), \\
E_l(z) - E_l(0) = E_{l_n}(z) - \mathcal{B}_{3n}(z), \\
I(z) - I(0) = I_n(z) - \mathcal{B}_{4n}(z), \\
T(z) - T(0) = T_n(z) - \mathcal{B}_{5n}(z), \\
G(z) - G(0) = G_n(z) - \mathcal{B}_{6n}(z), \\
L_r(z) - L_r(0) = L_{r_n}(z) - \mathcal{B}_{7n}(z), \\
R(z) - R(0) = R_n(z) - \mathcal{B}_{8n}(z).
\end{cases}
$$

Thus, using the triangular inequality with $\mathcal{A}_1$, we have

$$
\begin{aligned}
\|\mathcal{B}_{1n}(z)\| &= \|\frac{1}{\Gamma(\vartheta)} \int_0^z (z-y)^{\vartheta-1} \Big[\mathcal{A}_1(y, S(y)) - \mathcal{A}_1(y, S_{n-1}(y))\Big] dy\|, \\
&\leq \frac{1}{\Gamma(\vartheta)} \int_0^z (z-y)^{\vartheta-1} \Big[\|\mathcal{A}_1(y, S(y)) - \mathcal{A}_1(y, S_{n-1}(y))\|\Big] dy, \\
&\leq \frac{\gamma_1}{\Gamma(\vartheta)} z \|S - S_{n-1}\|.
\end{aligned}
$$

By using recursive principle, gives,

$$
\|\mathcal{B}_{1n}(z)\| \leq (\frac{\gamma_1}{\Gamma(\vartheta)} z)^{n+1} a.
$$

At z_0, we have

$$
\|\mathcal{B}_{1n}(z_0)\| \leq (\frac{\gamma_1}{\Gamma(\vartheta)} z_0)^{n+1} a.
$$

Hence,

$$
\|\mathcal{B}_{1n}(z)\| \to 0, \ \ as \ n \to \infty.
$$

Similarly,

$$
\|\mathcal{B}_{in}(z)\| \to 0, \ \ as \ n \to \infty, \ \ i = 2, \ldots, 8.
$$

Thus, the Model (2) has at least one solution. $\square$

Theorem 3.3. *The proposed Model* (2) *has one unique solution if,*

$$
1 - \frac{\gamma_i}{\Gamma(\vartheta)} z > 0, \ \forall \ i = 1, \ldots, 8.
$$

Proof. To show the uniqueness of solution of Model (2), let

$$
S(z) - S_1(z) = \frac{1}{\Gamma(\vartheta)} \int_0^z (z-y)^{\vartheta-1} [\mathcal{A}_1(y, S(y)) - \mathcal{A}_1(y, S_1(y))] dy. \tag{10}
$$

It is obvious that,

$$
\|S(z) - S_1(z)\| \geq 0. \tag{11}
$$

Taking norm on both sides of (10), yields,

$$\|S(z) - S_1(z)\| \le \frac{1}{\Gamma(\vartheta)} \int_0^z (z-y)^{\vartheta-1}[\|\mathcal{A}_1(y, S(y)) - \mathcal{A}_1(y, S_1(y))\|]dy.$$

Applying the Lipschitz condition on the kernel, we have

$$\|S(z) - S_1(z)\| \le (\frac{\gamma_1}{\Gamma(\vartheta)}z)\|S(z) - S_1(z)\|,$$

$$\|S(z) - S_1(z)\|(1 - \frac{\gamma_1}{\Gamma(\vartheta)}z) \le 0,$$

since,

$$1 - \frac{\gamma_1}{\Gamma(\vartheta)}z > 0,$$

we have

$$\|S(z) - S_1(z)\| = 0,$$
$$S(z) = S_1(z).$$

Similarly,

$$\begin{cases} E_e(z) = E_{e_1}(z), & E_l(z) = E_{l_1}(z), \\ I(z) = I_1(z), & T(z) = T_1(z), \\ G(z) = G_1(z), & L_r(z) = L_{r_1}(z), \\ R(z) = R_1(z). \end{cases}$$

Hence, Model (2) has a unique solution.   □

3.2   Positivity and boundedness

In this section, we analyze the positivity and boundedness of Model (2) to ensure that the model is well–posed.

Let the functions on the right hand side of Model (2) be continuous on R_+^8. The net population becomes,

$${}^C D^\vartheta N(z) = {}^C D^\vartheta S + {}^C D^\vartheta E_e + {}^C D^\vartheta E_l + {}^C D^\vartheta I + {}^C D^\vartheta T + {}^C D^\vartheta G + {}^C D^\vartheta L_r + {}^C D^\vartheta R,$$

which gives,

$${}^C D^\vartheta N(z) + \mu N(z) \le \Lambda. \tag{12}$$

Applying the Laplace transformation to (12), we have

$$N(z) \le \frac{\Lambda}{\mu}, \ \forall z.$$

Therefore, all the solutions of the given model restricted to the domain Ω. Now, to check all the solutions of the proposed Model (2) are positive, we observe that,

$$
\begin{cases}
{}^{C}D^{\vartheta}S = \Lambda > 0, \\
{}^{C}D^{\vartheta}E_e = \beta SI + \eta G \geq 0, \\
{}^{C}D^{\vartheta}E_l = kE_1 + q\eta G \geq 0, \\
{}^{C}D^{\vartheta}I = pkE_1 + \omega E_1 + \sigma\rho T \geq 0, \\
{}^{C}D^{\vartheta}T = rI \geq 0, \\
{}^{C}D^{\vartheta}G = \gamma T \geq 0, \\
{}^{C}D^{\vartheta}L_r = \sigma T + mE_e \geq 0, \\
{}^{C}D^{\vartheta}R = \xi T \geq 0.
\end{cases}
\tag{13}
$$

By Corollary 2.1, we conclude that the result is in R_+^8 i.e.,

$$
\Omega = \Big\{ \big(S, E_e, E_l, I, T, G, L_r, R\big) \in R_+^8 \mid \big(S + E_e + E_l + I + T + G + L_r + R\big) \geq 0 \Big\}.
$$

Hence, the solution of Model (2) are positive and bounded in the feasible region Ω.

3.3　Equilibrium analysis

3.3.1　Disease free equilibrium E_0

Let, ${}^{C}D^{\vartheta}S ={}^{C} D^{\vartheta}E_e ={}^{C} D^{\vartheta}E_l ={}^{C} D^{\vartheta}I ={}^{C} D^{\vartheta}T ={}^{C} D^{\vartheta}G ={}^{C} D^{\vartheta}L_r ={}^{C} D^{\vartheta}R = 0$, and from Model (2), we have

$$
\begin{cases}
\Lambda + \theta R - \beta SI - \mu S = 0, \\
\beta SI + k_1 G - k_2 E_e = 0, \\
k_3 E_e + q\eta G - k_4 E_l = 0, \\
pkE_e + \omega E_l - k_5 I + \sigma\rho T = 0, \\
rI - k_6 T = 0, \\
\gamma T - k_7 G = 0, \\
k_8 T + mE_e - \mu L_r = 0, \\
\xi T - k_9 R = 0.
\end{cases}
\tag{14}
$$

Put $E_e = E_l = I = T = G = L_r = 0$ in (14), gives $S = \dfrac{\Lambda}{\mu}$ and $R = 0$. Disease free equilibrium point (DFEP) is obtainable as;

$$
\mathbf{E_0} = \left(\frac{\Lambda}{\mu}, 0, 0, 0, 0, 0, 0, 0 \right).
$$

3.3.2　Basic reproduction number R_0

The R_0 of the presented Model (2) is determined through the utilization of the next–generation matrix scheme [51]. To compute R_0, examine the reduced system $X = (E_e, E_l, I, T, G, L_r)^T$, and

derive the required matrices $\mathcal{F}$ and $\mathcal{V}$ as,

$$
\mathcal{F} = \begin{bmatrix}
0 & 0 & \beta S & 0 & 0 & 0 \\
0 & 0 & 0 & 0 & 0 & 0 \\
0 & 0 & 0 & 0 & 0 & 0 \\
0 & 0 & 0 & 0 & 0 & 0 \\
0 & 0 & 0 & 0 & 0 & 0 \\
0 & 0 & 0 & 0 & 0 & 0
\end{bmatrix}, \qquad
\mathcal{V} = \begin{bmatrix}
k_2 E_e & 0 & 0 & 0 & -k_1 G & 0 \\
-k_3 E_e & k_4 E_l & 0 & 0 & -q\eta G & 0 \\
-pk E_e & -\omega E_l & k_5 I & -\sigma\rho T & 0 & 0 \\
0 & 0 & -rI & k_6 T & 0 & 0 \\
0 & 0 & 0 & -\gamma T & k_7 G & 0 \\
-m E_e & 0 & 0 & -k_8 T & 0 & \mu L_r
\end{bmatrix}.
$$

The Jacobian matrices computed at $\mathbf{E_0}$ are as follows:

$$
\mathcal{F}(\mathbf{E_0}) = \begin{bmatrix}
0 & 0 & \beta\frac{\Lambda}{\mu} & 0 & 0 & 0 \\
0 & 0 & 0 & 0 & 0 & 0 \\
0 & 0 & 0 & 0 & 0 & 0 \\
0 & 0 & 0 & 0 & 0 & 0 \\
0 & 0 & 0 & 0 & 0 & 0 \\
0 & 0 & 0 & 0 & 0 & 0
\end{bmatrix}, \qquad
\mathcal{V} = \begin{bmatrix}
k_2 & 0 & 0 & 0 & -k_1 & 0 \\
-k_3 & k_4 & 0 & 0 & -q\eta & 0 \\
-pk & -\omega & k_5 & -\sigma\rho & 0 & 0 \\
0 & 0 & -r & k_6 & 0 & 0 \\
0 & 0 & 0 & -\gamma & k_7 & 0 \\
-m & 0 & 0 & -k_8 & 0 & \mu
\end{bmatrix}.
$$

Now, from simplification of $\mathcal{F}\mathcal{V}^{-1}$, we have

$$
R_0 = \frac{(\omega k_3 + kpk_4)\Lambda\beta k_6 k_7}{k_2 k_4 k_5 k_6 k_7 \mu - k_2 k_4 k_7 r\sigma\rho\mu - k_2 qr\mu\gamma\omega\eta - (\omega k_3 + pkk_4)k_1\mu r\gamma}.
$$

3.3.3 Disease endemic equilibrium $\mathbf{E^e}$

Let replace $S = S^*$, $E_e^* = E_e$, $E_l^* = E_l$, $I = I^*$, $T = T^*$, $G = G^*$, $L_r = L_r^*$, and $R = R^*$ in (14), and solve the respective quantity, we obtain

$$
S^* = \frac{\Lambda}{\mu R_0},
$$

$$
E_e^* = \frac{\left[k_4 k_7(k_5 k_6 - r\sigma\rho) - q\eta\omega\gamma r\right]\left(k_9 r\Lambda\mu(R_0 - 1)\right)}{\left[(\omega k_3 + pkk_4)k_7 r\right](\Lambda k_6 k_9 \beta - R_0 \mu\theta\xi r)},
$$

$$
E_l^* = \frac{\left[k_3 k_7(k_5 k_6 - r\sigma\rho) - pkq\eta r\gamma\right]\left(k_9 r\Lambda\mu(R_0 - 1)\right)}{\left[k_7 r(\omega k_3 + pkk_4)\right](\Lambda k_6 k_9 \beta - R_0 \mu\theta\xi r)},
$$

$$
I^* = \frac{k_9 k_6 r\Lambda\mu(R_0 - 1)}{\Lambda k_6 k_9 \beta - R_0 \mu\theta\xi r^2},
$$

$$
T^* = \frac{k_9 r\Lambda\mu(R_0 - 1)}{\Lambda k_6 k_9 \beta - R_0 \mu\theta\xi r},
$$

$$
G^* = \frac{k_9 r\gamma\Lambda\mu(R_0 - 1)}{\Lambda k_6 k_9 \beta - R_0 \mu\theta\xi r k_7},
$$

$$
L_r^* = \frac{\left[mk_4 k_7(k_5 k_6 - r\sigma\rho) - (wk_3 + pkk_4)(k_7 k_8 r) - q\eta\omega r\gamma m\right](k_9 r\Lambda\mu(R_0 - 1))}{\left[k_7 r\mu(wk_3 + pkk_4)\right](\Lambda k_6 k_9 \beta - R_0 \mu\theta\xi r)},
$$

$$
R^* = \frac{k_9 r\xi\Lambda\mu(R_0 - 1)}{\Lambda k_6 k_9^2 \beta - R_0 \mu\theta\xi r}.
$$

4   Stability Analysis

In this section, we analyze the stability of the equilibria by formulating the Jacobian matrix. The purpose of analyzing the stability of fractional–order systems is to ensure the reliability and predictability of the model's behavior, which is crucial for applications in various fields, including biology and epidemiology.

Theorem 4.1. *The disease free equilibrium point* (*DFEP*) $\mathbf{E_0}$ *of Model* (2) *is locally asymptotically stable* (*LAS*) *if* $R_0 < 1$ *and* $A < B$.

Proof. The DFEP is LAS if all the eigenvalues λ_i, $i = 1, \ldots, 8$ of the Jacobian matrix $\mathbf{J}(\mathbf{E_0})$ satisfies the following conditions;

$$|arg(\lambda_i)| > \frac{\vartheta\pi}{2}.$$

Insert $\mathbf{E_0}$, then the Jacobian matrix gives,

$$\mathbf{J}(\mathbf{E_0}) = \begin{bmatrix} -\mu & 0 & 0 & -\frac{\beta\Lambda}{\mu} & 0 & 0 & 0 & \theta \\ 0 & -k_2 & 0 & \frac{\beta\Lambda}{\mu} & 0 & k_1 & 0 & 0 \\ 0 & k_3 & -k_4 & 0 & 0 & q\eta & 0 & 0 \\ 0 & pk & \omega & -k_5 & 0 & 0 & 0 & 0 \\ 0 & 0 & 0 & r & -k_6 & 0 & 0 & 0 \\ 0 & 0 & 0 & 0 & \gamma & -k_7 & 0 & 0 \\ 0 & m & 0 & 0 & k_8 & 0 & -\mu & 0 \\ 0 & 0 & 0 & 0 & \xi & 0 & 0 & -k_9 \end{bmatrix}.$$

Clearly, we get $\lambda_1 = -\mu$, $\lambda_2 = -k_9$, while the remaining eigenvalues can be obtained from the reduced matrix,

$$\mathbf{J_3} = \begin{bmatrix} -k_2 & 0 & \frac{\beta\Lambda}{\mu} & 0 & k_1 & 0 \\ k_3 & -k_4 & 0 & 0 & q\eta & 0 \\ pk & \omega & -k_5 & 0 & 0 & 0 \\ 0 & 0 & r & -k_6 & 0 & 0 \\ 0 & 0 & 0 & \gamma & -k_7 & 0 \\ m & 0 & 0 & k_8 & 0 & -\mu \end{bmatrix},$$

the trace and the determinant of $\mathbf{J_3}$ are

$$tr(\mathbf{J_3}) = -k_2 k_4 k_5 k_6 k_7 \mu < 0, \quad \text{and} \quad \det(\mathbf{J_3}) = B - A,$$

where

$$B = \mu k_2 k_4 k_5 k_6 k_7, \quad A = r\gamma\omega k_1 k_3 + qr\gamma\mu\nu\omega k_2 + r\sigma\mu\rho k_2 k_4 k_7 + \Lambda\beta\omega k_3 k_6 k_7.$$

Thus, $\det(\mathbf{J_3}) > 0$, if $A < B$, and all the eigenvalues of Jacobian matrix satisfy $|arg(\lambda_i)| > \frac{\vartheta\pi}{2}$ if and only if $R_0 < 1$, which provides $\mathbf{E_0}$ is LAS. $\square$

Theorem 4.2. *The disease endemic equilibrium point* (*DEEP*) $\mathbf{E^e}$ *of Model* (2) *is globally asymptotically stable* (*GAS*) *if* $R_0 > 1$.

Proof. Let

$$
\begin{aligned}
F(z) = \frac{1}{2}\Big[& (S - S^*)^2 + (E_e - E_e^*)^2 + (E_l - E_l^*)^2 + (I - I^*)^2 \\
& + (T - T^*)^2 + (G - G^*)^2 + (L_r - L_r^*)^2 + (R - R^*)^2 \Big],
\end{aligned}
\tag{15}
$$

be well defined, continuous and positive definite for all initial condition. Applying the Caputo fractional derivative on both sides of (15), we have

$$
\begin{aligned}
{}^C D^\vartheta F(z) \leq {} & (S - S^*)\,{}^C D^\vartheta(S - S^*) + (E_e - E_e^*)\,{}^C D^\vartheta(E_e - E_e^*) + (E_l - E_l^*)\,{}^C D^\vartheta(E_l - E_l^*) \\
& + (I - I^*)\,{}^C D^\vartheta(I - I^*) + (T - T^*)\,{}^C D^\vartheta(T - T^*) + (G - G^*)\,{}^C D^\vartheta(G - G^*) \\
& + (L_r - L_r^*)\,{}^C D^\vartheta(L_r - L_r^*) + (R - R^*)\,{}^C D^\vartheta(R - R^*),
\end{aligned}
$$

which gives

$$
\begin{aligned}
{}^C D^\vartheta F(z) \leq {} & (S - S^*)\,{}^C D^\vartheta S + (E_e - E_e^*)\,{}^C D^\vartheta E_e + (E_l - E_l^*)\,{}^C D^\vartheta E_l + (I - I^*)\,{}^C D^\vartheta I \\
& + (T - T^*)\,{}^C D^\vartheta T + (G - G^*)\,{}^C D^\vartheta G + (L_r - L_r^*)\,{}^C D^\vartheta L_r + (R - R^*)\,{}^C D^\vartheta R.
\end{aligned}
$$

Using (2), we obtain

$$
\begin{aligned}
{}^C D^\vartheta F(z) \leq {} & (S - S^*)[\Lambda + \theta R - \beta SI - \mu S] + (E_e - E_e^*)[\beta SI + k_1 G - k_2 E_e] \\
& + (E_l - E_l^*)[k_3 E_e + q\eta G - k_4 E_l] + (I - I^*)[pk E_e + \omega E_l - k_5 I + \sigma\rho T] \\
& + (T - T^*)[rI - k_6 T] + (G - G^*)[\gamma T - k_7 G] + (L_r - L_r^*)[k_8 T + m E_e - \mu L_r] \\
& + (R - R^*)[\xi T - k_9 R],
\end{aligned}
$$

and

$$
\begin{aligned}
{}^C D^\vartheta F(z) \leq {} & \Lambda S + \theta RS + \beta S S^* I + \mu S S^* - \beta S^2 I - \mu S^2 - \Lambda S^* - \theta R S^* + \beta S I E_e + k_1 G E_e \\
& + k_2 E_e E_e^* - k_2 E_e^2 - \beta S I E_e^* - k_1 G E_e^* + k_3 E_e E_l + q\eta G E_l + k_4 E_l E_l^* - k_4 E_l^2 \\
& - k_3 E_e E_l^* - q\eta G E_l^* + pk E_e I + \omega E_l I + \sigma\rho T I + k_5 I I^* + k_6 T T^* - k_5 I^2 - pk E_e I^* \\
& - \omega E_l I^* - k_6 T^2 - r I T + r T G + k_7 G G^* - k_7 G^2 - \gamma T G^* + k_8 T L_r + m E_e L_r \\
& + \mu L_r L_r^* - \mu L_r^2 - k_8 T L_r^* - m E_e L_r^* + \xi T R + k_9 R R^* - k_9 R^2 - \xi T R^*,
\end{aligned}
$$

which implies that,

$$
{}^C D^\vartheta F(z) \leq Y - X,
$$

where

$$
\begin{aligned}
Y = \Big[& \Lambda S + \theta RS + \beta S S^* I + \mu S S^* + \beta S I E_e + k_1 G E_e + k_2 E_e E_e^* + k_3 E_e E_l \\
& + q\eta G E_l + k_4 E_l E_l^* + pk E_e I + \omega E_l I + \sigma\rho T I + k_5 I I^* + r I T + k_6 T T^* \\
& + r T G + k_7 G G^* + k_8 T L_r + m E_e L_r + \mu L_r L_r^* + \xi T R + k_9 R R^* \Big], \\
X = \Big[& \beta S^2 I + \mu S^2 + \Lambda S^* + \theta R S^* + k_2 E_e^2 + \beta S I E_e^* + k_1 G E_e^* + k_4 E_l^2 + k_3 E_e E_l^* \\
& + q\eta G E_l^* + k_5 I^2 - pk E_e I^* + \omega E_l I^* + k_6 T^2 + r I T^* + k_7 G^2 + \gamma T G^* + \mu L_r^2 \\
& + k_8 T L_r^* + m E_e L_r^* + k_9 R^2 + \xi T R^* \Big].
\end{aligned}
$$

Thus, ${}^C D^\vartheta F(z) \leq 0$, if $Y < X$ and if $S = S^*$, $E_e = E_e^*$, $E_l = E_l^*$, $I = I^*$, $T = T^*$, $G = G^*$, $L_r = L_r^*$, $R = R^*$ then ${}^C D^\vartheta F(z) = 0$. Therefore, F is Lyapunov function on the feasible region $\{S, E_e, E_l, I, T, G, L_r, R \in R^8, {}^C D^\vartheta F = 0\}$ and the largest set $\{S^*, E_e^*, E_l^*, I^*, T^*, G^*, L_r^*, R^*\}$ in the feasible region is singleton. Hence $\mathbf{E}^e$ is GAS, if all these conditions and $R_0 \geq 1$ holds. □

5 Sensitivity Analysis

The sensitivity analysis of the basic reproduction number R_0 is carried out by calculating the sensitivity index of each parameter. This sensitivity index quantifies the relative change in basic reproduction number when a parameter value changes. We employ a similar method to Tilahun et al. [45] to compute the normalized forward sensitivity index of basic reproduction number with respect to a particular parameter. The sensitivity index of R_0 with respect to the model parameters are given by,

$$\Upsilon_k^{R_0} = \frac{k(\omega - p\omega + pk_4)}{A} - \frac{k}{B}\left[k_4 k_7(k_5 k_6 - r\sigma\rho) - r\gamma\left(pk_1(k_4 - \omega) - \omega(q\eta + k_1)\right)\right],$$

$$\Upsilon_\mu^{R_0} = \mu\left[\frac{k_6 + k_7}{k_6 k_7} + \frac{kp}{A} - \frac{(k_5 k_6 k_7(k_4 + k_2) + k_2 k_4(k_5 k_6 + k_5 k_7 + k_6 k_7)}{B}\right.$$
$$\left. - \frac{(r\sigma\rho(k_2(k_4 + k_7) + k_4 k_7) + r\gamma(q\omega\eta + pkk_1))}{B} - 1\right],$$

$$\Upsilon_\omega^{R_0} = \frac{\Lambda\beta k_6 k_7}{\mu B}\left[k_3 + kp - \frac{A}{B}(k_2 k_5 k_6 k_7 - k_2 k_7 r\sigma\rho - k_2 qr\gamma\eta - (k_3 + pk)k_1 r\gamma)\right],$$

$$\Upsilon_p^{R_0} = pk(k_4 - \omega)\left[\frac{1}{A} - \frac{k_1 r\gamma}{B}\right], \qquad \Upsilon_r^{R_0} = \frac{r(k_2 k_4 k_7(\sigma\rho - k_6) + \gamma(k_2 q\omega\eta + Ak_1))}{B},$$

$$\Upsilon_{d_1}^{R_0} = -\frac{k_2 k_4 k_6 k_7 d_1}{B}, \qquad \Upsilon_\sigma^{R_0} = \frac{\sigma}{k_6} - \frac{\sigma k_2 k_4 k_7 k_6 + k_5 - r\rho}{B}, \qquad \Upsilon_\rho^{R_0} = \frac{k_2 k_4 k_7 r\rho\sigma}{B},$$

$$\Upsilon_\eta^{R_0} = \frac{A\Lambda\beta k_6}{\mu B}\left(1 - \frac{k_7(k_2 k_4(k_5 k_6 - r\sigma\rho) - r\gamma(k_2 q\omega + (1 - q)A))}{B}\right), \qquad \Upsilon_\Lambda^{R_0} = 1,$$

$$\Upsilon_{d_2}^{R_0} = \frac{d_2}{k_6} - \frac{k_2 k_4 k_5 k_7 d_2}{B}, \qquad \Upsilon_\gamma^{R_0} = \frac{\gamma}{k_6} - \frac{\gamma(k_2 k_4 k_5 k_7 - k_2 qr\omega\eta - Ak_1 r)}{B},$$

$$\Upsilon_\xi^{R_0} = \frac{\xi}{k_6} - \frac{k_2 k_4 k_5 k_7 \xi}{B}, \qquad \Upsilon_{d_3}^{R_0} = \frac{d_3}{k_7} - \frac{k_2 k_4 d_3(k_5 k_6 - r\sigma\rho)}{B}, \qquad \Upsilon_\beta^{R_0} = 1,$$

$$\Upsilon_m^{R_0} = \frac{m(k_4 k_7(r\sigma\rho - k_5 k_6) + qr\gamma\omega\eta)}{B}, \qquad \Upsilon_q^{R_0} = \frac{qr\gamma\eta(k_2\omega - A)}{B},$$

where $A = \omega k_3 + kpk_4$, $B = k_2 k_4 k_7(k_5 k_6 - r\sigma\rho) - k_2 qr\gamma\omega\eta - Ak_1 r\gamma$. The sensitivity index's sign for each parameter is presented in Table 2.

Table 2: Sensitivity index's sign for each parameter.

Parameter	Sign	Parameter	Sign	Parameter	Sign	Parameter	Sign	Parameter	Sign
μ	-	p	-	k	-	d_2	-	γ	-
d_3	-	r	-	σ	+	ω	+	β	+
m	+	ξ	+	d_1	+	η	+	ρ	+
Λ	+	q	+						

The parameters ω, Λ, β, ξ, σ, η, m, d_1, ρ, and q are associated with positive indices, while p, k, μ, d_2, γ, d_3, and r exhibit negative indices. Parameters with positive indices play a pivotal role in the disease's expansion within the population, leading to an increase in the basic reproduction number with their rising values. Conversely, parameters with negative indices contribute to the disease's elimination within the population, emphasizing the importance of increasing their values for disease eradication. It is worth noting that the sensitivity index might be a complex expression, contingent on different system parameters, but it can also be a constant value independent of specific parameter values. For example, $\Upsilon_\beta^{R_0} = 1$ and $\Upsilon_\Lambda^{R_0} = 1$.

Figure 2 shows a graphical view of infected individuals verses time (weeks) with the variation of σ. All the used parameters are exhibit in Table 3. The obtained figure corroborates the sensitivity index σ. It illustrates the number of the infected human population based on the parameter values provided in Table 3, alongside a corresponding plot reflecting 75% increment in the parameter value. The figure shows that if we increase the value of σ from 0.15 to 0.9, then we get small changes of increment of the infected population. After 12 weeks, we observe that both graphs coincides each other. After 45 weeks, both graphs show stability and convergence. All the remaining parameters exhibit minimal impact on R_0, with changes that are not visually discernible in the graphs. Consequently, the graphs for these parameters are omitted.
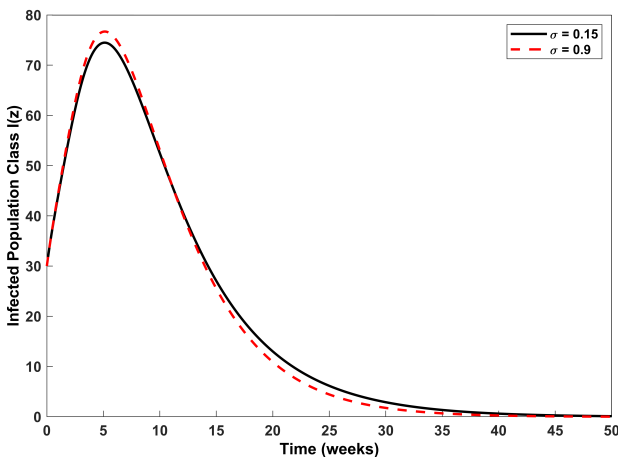

Figure 2: Effect of $I(z)$ verses time (weeks) with the variation of σ.

6   Numerical Analysis

6.1   General solution of Model (2) by LADM

In this section, we apply the Laplace Adomian decomposition method (LADM) on Model (2) with initial conditions. Let $S(0) = N_1 > 0$, $E_e(0) = N_2 > 0$, $E_l(0) = N_3 > 0$, $I(0) = N_4 > 0$, $T(0) = N_5 > 0$, $G(0) = N_6 > 0$, $L_r(0) = N_7 > 0$, $R(0) = N_8 > 0$. Taking the Laplace transform of

Model (2), gives,

$$
\begin{cases}
\mathsf{L}[S(z)] = \dfrac{N_1}{s} + \dfrac{1}{s^{\vartheta}}\mathsf{L}\big[\Lambda + \theta R - \beta SI - \mu S\big], \\[2mm]
\mathsf{L}[E_e(z)] = \dfrac{N_2}{s} + \dfrac{1}{s^{\vartheta}}\mathsf{L}\big[\beta SI + k_1 G - k_2 E_e\big], \\[2mm]
\mathsf{L}[E_l(z)] = \dfrac{N_3}{s} + \dfrac{1}{s^{\vartheta}}\mathsf{L}\big[k_3 E_e + q\eta G - k_4 E_l\big], \\[2mm]
\mathsf{L}[I(z)] = \dfrac{N_4}{s} + \dfrac{1}{s^{\vartheta}}\mathsf{L}\big[pk E_e + \omega E_l - k_5 I + \sigma\rho T\big], \\[2mm]
\mathsf{L}[T(z)] = \dfrac{N_5}{s} + \dfrac{1}{s^{\vartheta}}\mathsf{L}\big[rI - k_6 T\big], \\[2mm]
\mathsf{L}[G(z)] = \dfrac{N_6}{s} + \dfrac{1}{s^{\vartheta}}\mathsf{L}\big[\gamma T - k_7 G\big], \\[2mm]
\mathsf{L}[L_r(z)] = \dfrac{N_7}{s} + \dfrac{1}{s^{\vartheta}}\mathsf{L}\big[k_8 T + m E_e - \mu L_r\big], \\[2mm]
\mathsf{L}[R(z)] = \dfrac{N_8}{s} + \dfrac{1}{s^{\vartheta}}\mathsf{L}\big[\xi T - k_9 R\big].
\end{cases}
\tag{16}
$$

Let the solution of Model (2) be written as an infinite series for S, E_e, E_l, I, T, G, L_r, R given by,

$$
\begin{cases}
S(z) = \sum\limits_{n=0}^{\infty} S_n(z), \quad E_e(z) = \sum\limits_{n=0}^{\infty} E_{e_n}(z), \quad E_l(z) = \sum\limits_{n=0}^{\infty} E_{l_n}(z), \quad I(z) = \sum\limits_{n=0}^{\infty} I_n(z), \\[3mm]
T(z) = \sum\limits_{n=0}^{\infty} T_n(z), \quad G(z) = \sum\limits_{n=0}^{\infty} G_n(z), \quad L_r(z) = \sum\limits_{n=0}^{\infty} L_{r_n}(z), \quad R(z) = \sum\limits_{n=0}^{\infty} R_n(z).
\end{cases}
\tag{17}
$$

The non linearity $S(z)I(z)$ can be written as,

$$
S(z)I(z) = \sum_{n=0}^{\infty} X_n(z),
$$

where $X_n(z)$ is called the Adomian polynomials given as,

$$
X_n(z) = \frac{1}{n!}\frac{d^n}{d\lambda^n}\left[\sum_{i=0}^{n}\lambda^i S_i(z)\sum_{i=0}^{n}\lambda^i I_i(z)\right]_{\lambda=0}.
\tag{18}
$$

Substitute (17) and (18) in (16), yields

$$
\begin{cases}
\mathsf{L}[S_0(z)] = \dfrac{N_1}{s}, \quad \mathsf{L}[E_{e_0}(z)] = \dfrac{N_2}{s}, \quad \mathsf{L}[E_{l_0}(z)] = \dfrac{N_3}{s}, \quad \mathsf{L}[I_0(z)] = \dfrac{N_4}{s}, \\[3mm]
\mathsf{L}[T_0(z)] = \dfrac{N_5}{s}, \quad \mathsf{L}[G_0(z)] = \dfrac{N_6}{s}, \quad \mathsf{L}[L_{r_0}(z)] = \dfrac{N_7}{s}, \quad \mathsf{L}[R_0(z)] = \dfrac{N_8}{s},
\end{cases}
\tag{19}
$$

and

$$
\begin{cases}
\mathsf{L}[S_1(z)] = \dfrac{1}{s^\vartheta}\mathsf{L}\big[\Lambda + \theta R_0 - \beta X_0 - \mu S_0\big], \\[2mm]
\mathsf{L}[E_{e_1}(z)] = \dfrac{1}{s^\vartheta}\mathsf{L}\big[\beta X_0 + k_1 G_0 - k_2 E_{e_0}\big], \\[2mm]
\mathsf{L}[E_{l_1}(z)] = \dfrac{1}{s^\vartheta}\mathsf{L}\big[k_3 E_{e_0} + q\eta G_0 - k_4 E_{l_0}\big], \\[2mm]
\mathsf{L}[I_1(z)] = \dfrac{1}{s^\vartheta}\mathsf{L}\big[pk E_{e_0} + \omega E_{l_0} - k_5 I_0 + \sigma\rho T_0\big], \\[2mm]
\mathsf{L}[T_1(z)] = \dfrac{1}{s^\vartheta}\mathsf{L}\big[r I_0 - k_6 T_0\big], \\[2mm]
\mathsf{L}[G_1(z)] = \dfrac{1}{s^\vartheta}\mathsf{L}\big[\gamma T_0 - k_7 G_0\big], \\[2mm]
\mathsf{L}[L_{r_1}(z)] = \dfrac{1}{s^\vartheta}\mathsf{L}\big[k_8 T_0 + m E_{e_0} - \mu L_{r_0}\big], \\[2mm]
\mathsf{L}[R_1(z)] = \dfrac{1}{s^\vartheta}\mathsf{L}\big[\xi T_0 - k_9 R_0\big], \\[2mm]
\;\;\vdots \\[2mm]
\mathsf{L}[S_{n+1}(z)] = \dfrac{1}{s^\vartheta}\mathsf{L}\big[\Lambda + \theta R_n - \beta X_n - \mu S_n\big], \\[2mm]
\mathsf{L}[E_{e_{n+1}}(z)] = \dfrac{1}{s^\vartheta}\mathsf{L}\big[\beta X_n + k_1 G_n - k_2 E_{e_n}\big], \\[2mm]
\mathsf{L}[E_{l_{n+1}}(z)] = \dfrac{1}{s^\vartheta}\mathsf{L}\big[k_3 E_{e_n} + q\eta G_n - k_4 E_{l_n}\big], \\[2mm]
\mathsf{L}[I_{n+1}(z)] = \dfrac{1}{s^\vartheta}\mathsf{L}\big[pk E_{e_n} + \omega E_{l_n} - k_5 I_n + \sigma\rho T_n\big], \\[2mm]
\mathsf{L}[T_{n+1}(z)] = \dfrac{1}{s^\vartheta}\mathsf{L}\big[r I_n - k_6 T_n\big], \\[2mm]
\mathsf{L}[G_{n+1}(z)] = \dfrac{1}{s^\vartheta}\mathsf{L}\big[\gamma T_n - k_7 G_n\big], \\[2mm]
\mathsf{L}[L_{r_{n+1}}(z)] = \dfrac{1}{s^\vartheta}\mathsf{L}\big[k_8 T_n + m E_{e_n} - \mu L_{r_n}\big], \\[2mm]
\mathsf{L}[R_{n+1}(z)] = \dfrac{1}{s^\vartheta}\mathsf{L}\big[\xi T_n - k_9 R_n\big].
\end{cases}
\tag{20}
$$

Applying the Laplace inverse transform to (19) and (20), gives

$$
\begin{cases}
S_0(z) = \mathsf{L}^{-1}\!\left[\dfrac{N_1}{s}\right] = N_1, \quad E_{e_0}(z) = \mathsf{L}^{-1}\!\left[\dfrac{N_2}{s}\right] = N_2, \quad E_{l_0}(z) = \mathsf{L}^{-1}\!\left[\dfrac{N_3}{s}\right] = N_3, \\[3mm]
I_0(z) = \mathsf{L}^{-1}\!\left[\dfrac{N_4}{s}\right] = N_4, \quad T_0(z) = \mathsf{L}^{-1}\!\left[\dfrac{N_5}{s}\right] = N_5, \quad G_0(z) = \mathsf{L}^{-1}\!\left[\dfrac{N_6}{s}\right] = N_6, \\[3mm]
L_{r_0}(z) = \mathsf{L}^{-1}\!\left[\dfrac{N_7}{s}\right] = N_7 \quad R_0(z) = \mathsf{L}^{-1}\!\left[\dfrac{N_8}{s}\right] = N_8.
\end{cases}
$$

$$
\begin{cases}
S_1(z) = \left[\Lambda + \theta N_8 - \beta N_1 N_4 - \mu N_1\right]\dfrac{z^\vartheta}{\Gamma(\vartheta+1)}, \\[2mm]
E_{e_1}(z) = \left[\beta N_1 N_4 + k_1 N_6 - k_2 N_2\right]\dfrac{z^\vartheta}{\Gamma(\vartheta+1)}, \\[2mm]
E_{l_1}(z) = \left[k_3 N_2 + q\eta N_6 - k_4 N_3\right]\dfrac{z^\vartheta}{\Gamma(\vartheta+1)}, \\[2mm]
I_1(z) = \left[pk N_2 + \omega N_3 - k_5 N_4 + \sigma\rho N_5\right]\dfrac{z^\vartheta}{\Gamma(\vartheta+1)}, \\[2mm]
T_1(z) = \left[r N_4 - k_6 N_5\right]\dfrac{z^\vartheta}{\Gamma(\vartheta+1)}, \\[2mm]
G_1(z) = \left[\gamma N_5 - k_7 N_6\right]\dfrac{z^\vartheta}{\Gamma(\vartheta+1)}, \\[2mm]
L_{r_1}(z) = \left[k_8 N_5 + m N_2 - \mu N_7\right]\dfrac{z^\vartheta}{\Gamma(\vartheta+1)}, \\[2mm]
R_1(z) = \left[\xi N_5 - k_9 N_8\right]\dfrac{z^\vartheta}{\Gamma(\vartheta+1)}.
\end{cases}
$$

$$
\begin{cases}
S_2(z) = \dfrac{\Lambda z^\vartheta}{\Gamma(\vartheta+1)} + \left[\theta b_{11} - \beta(N_1 x_{11} + N_4 v_{11}) - \mu v_{11}\right]\dfrac{z^{2\vartheta}}{\Gamma(2\vartheta+1)}, \\[2mm]
E_{e_2}(z) = \left[\beta(N_1 x_{11} + N_4 v_{11}) + k_1 z_{11} - k_2 u_{11}\right]\dfrac{z^{2\vartheta}}{\Gamma(2\vartheta+1)}, \\[2mm]
E_{l_2}(z) = \left[k_3 u_{11} + q\eta z_{11} - k_4 w_{11}\right]\dfrac{z^{2\vartheta}}{\Gamma(2\vartheta+1)}, \\[2mm]
I_2(z) = \left[pk u_{11} + \omega w_{11} - k_5 x_{11} + \sigma\rho y_{11}\right]\dfrac{z^{2\vartheta}}{\Gamma(2\vartheta+1)}, \\[2mm]
T_2(z) = \left[r x_{11} - k_6 y_{11}\right]\dfrac{z^{2\vartheta}}{\Gamma(2\vartheta+1)}, \\[2mm]
G_2(z) = \left[\gamma y_{11} - k_7 z_{11}\right]\dfrac{z^{2\vartheta}}{\Gamma(2\vartheta+1)}, \\[2mm]
L_{r_2}(z) = \left[k_8 y_{11} + m u_{11} - \mu a_{11}\right]\dfrac{z^{2\vartheta}}{\Gamma(2\vartheta+1)}, \\[2mm]
R_2(z) = \left[\xi y_{11} - k_9 b_{11}\right]\dfrac{z^{2\vartheta}}{\Gamma(2\vartheta+1)},
\end{cases}
$$

where

$$
\begin{cases}
v_{11} = \Lambda + \theta N_8 - \beta N_1 N_4 - \mu N_1, \\
u_{11} = \beta N_1 N_4 - k_1 N_6 - k_2 N_2, \\
w_{11} = k_3 N_2 + q\eta N_6 - k_4 N_3, \\
x_{11} = pk N_2 + \omega N_3 - k_5 N_4 + \sigma\rho N_5, \\
y_{11} = r N_4 - k_6 N_5, \qquad z_{11} = \gamma N_5 - k_7 N_6, \\
a_{11} = k_8 N_5 + m N_2 - \mu N_7, \qquad b_{11} = \xi N_5 - k_9 N_8.
\end{cases}
$$

Finally, we have

$$
\begin{cases}
llS(z) = N_1 + (v_{11} + \Lambda)\dfrac{z^\vartheta}{\Gamma(\vartheta + 1)} + v_{111}\dfrac{z^{2\vartheta}}{\Gamma(2\vartheta + 1)} + \ldots \\[2mm]
E_e(z) = N_2 + u_{11}\dfrac{z^\vartheta}{\Gamma(\vartheta + 1)} + u_{111}\dfrac{z^{2\vartheta}}{\Gamma(2\vartheta + 1)} + \ldots \\[2mm]
E_l(z) = N_3 + w_{11}\dfrac{z^\vartheta}{\Gamma(\vartheta + 1)} + w_{111}\dfrac{z^{2\vartheta}}{\Gamma(2\vartheta + 1)} + \ldots \\[2mm]
I(z) = N_4 + x_{11}\dfrac{z^\vartheta}{\Gamma(\vartheta + 1)} + x_{111}\dfrac{z^{2\vartheta}}{\Gamma(2\vartheta + 1)} + \ldots \\[2mm]
T(z) = N_5 + y_{11}\dfrac{z^\vartheta}{\Gamma(\vartheta + 1)} + y_{111}\dfrac{z^{2\vartheta}}{\Gamma(2\vartheta + 1)} + \ldots \\[2mm]
G(z) = N_6 + z_{11}\dfrac{z^\vartheta}{\Gamma(\vartheta + 1)} + z_{111}\dfrac{z^{2\vartheta}}{\Gamma(2\vartheta + 1)} + \ldots \\[2mm]
L_r(z) = N_7 + a_{11}\dfrac{z^\vartheta}{\Gamma(\vartheta + 1)} + a_{111}\dfrac{z^{2\vartheta}}{\Gamma(2\vartheta + 1)} + \ldots \\[2mm]
R(z) = N_8 + b_{11}\dfrac{z^\vartheta}{\Gamma(\vartheta + 1)} + b_{111}\dfrac{z^{2\vartheta}}{\Gamma(2\vartheta + 1)} + \ldots
\end{cases}
\tag{21}
$$

where

$$
\begin{cases}
v_{11} = \Lambda + \theta N_8 - \beta N_1 N_4 - \mu N_1, \quad u_{11} = \beta N_1 N_4 - k_1 N_6 - k_2 N_2, \\
w_{11} = k_3 N_2 + q\eta N_6 - k_4 N_3, \quad x_{11} = pk N_2 + \omega N_3 - k_5 N_4 + \sigma\rho N_5, \\
y_{11} = r N_4 - k_6 N_5, \quad z_{11} = \gamma N_5 - k_7 N_6, \quad a_{11} = k_8 N_5 + m N_2 - \mu N_7, \\
b_{11} = \xi N_5 - k_9 N_8, \quad v_{111} = \theta b_{11} - \beta(N_1 x_{11} + N_3 v_{11}) - \mu v_{11}, \\
u_{111} = \beta(N_1 x_{11} + N_3 v_{11}) + k_1 z_{11} - k_2 u_{11}, \quad w_{111} = k_3 u_{11} + q\eta z_{11} - k_4 w_{11}, \\
x_{111} = pk u_{11} + \omega w_{11} - k_5 x_{11} + \sigma\rho y_{11}, \quad y_{111} = r x_{11} - k_6 y_{11}, \quad z_{111} = \gamma y_{11} - k_7 z_{11}, \\
a_{111} = k_8 y_{11} + m u_{11} - \mu a_{11}, \quad b_{111} = \xi y_{11} - k_9 b_{11}.
\end{cases}
$$

In a similar fashion, the remaining terms of the series solution can be obtained.

Table 3: Parameters values (per year) of the TB model.

Parameter	Description	Value	Source
Λ	Recruitment rate	0.02	[19]
θ	Fraction of recovered individuals being suspected	0.5	Assumed
β	Rate of transmission from S to I	0.02	[14]
μ	Natural fatality rate	0.0143	[30]
q	Rate of self cured person from G enter into E_l	0.9	[30]
η	Rate of self cured persons in G due to immune system	0.2	[30]
m	Progression rate from E_e to L_r	0.2077	[26]
k	Reactivation rate of the early latent persons	0.08	[30]
p	Latent persons fast TB progression rate	0.075	[30]
ω	Reactivation rate of long term latent individuals	0.2	[30]
r	Rate of treatment for untreated active TB cases	0.3	[30]
d_1	Disease induced fatality rate in I	0.5	[30]
σ	Treatment rate	0.15	[19]
ρ	Treatment failure probability	0.2	[26]
d_2	Disease induced fatality rate in T	0.1	[30]
γ	Treatment rate interruption in class T	0.2	[30]
ξ	Recovery rate	0.1	[30]
d_3	Disease induced fatality rate in G	0.2	[30]

6.2 Numerical results

In this section, we present the numerical simulations of the proposed Model (2) using the LADM described above. Parameters values are given in Table 2, subject to the initial conditions [19] $N_1 = 1770$, $N_2 = 300$, $N_3 = 200$, $N_4 = 30$, $N_5 = 0$, $N_6 = 0$, $N_7 = 0.666$, and $N_8 = 0$, then from (21), we obtain

$$
\begin{cases}
S(z) = 1770 - 1087.271\dfrac{z^\vartheta}{\Gamma(\vartheta+1)} + 212.28\dfrac{z^{2\vartheta}}{\Gamma(2\vartheta+1)} + \dots \\[2mm]
E_e(z) = 300 + 971.4\dfrac{z^\vartheta}{\Gamma(\vartheta+1)} - 490.092\dfrac{z^{2\vartheta}}{\Gamma(2\vartheta+1)} + \dots \\[2mm]
E_l(z) = 200 - 20.66\dfrac{z^\vartheta}{\Gamma(\vartheta+1)} + 76.31\dfrac{z^{2\vartheta}}{\Gamma(2\vartheta+1)} + \dots \\[2mm]
I(z) = 30 + 12.871\dfrac{z^\vartheta}{\Gamma(\vartheta+1)} - 10.445\dfrac{z^{2\vartheta}}{\Gamma(2\vartheta+1)} + \dots \\[2mm]
T(z) = 9\dfrac{z^\vartheta}{\Gamma(\vartheta+1)} - 1.2174\dfrac{z^{2\vartheta}}{\Gamma(2\vartheta+1)} + \dots \\[2mm]
G(z) = 1.8\dfrac{z^{2\vartheta}}{\Gamma(2\vartheta+1)} + \dots \\[2mm]
L_r(z) = 0.666 + 62.30\dfrac{z^\vartheta}{\Gamma(\vartheta+1)} + 201.95\dfrac{z^{2\vartheta}}{\Gamma(2\vartheta+1)} + \dots \\[2mm]
R(z) = 0.9\dfrac{z^{2\vartheta}}{\Gamma(2\vartheta+1)} + \dots.
\end{cases}
\tag{22}
$$

We check all compartments of the proposed model to see how the model behaves dynamically at different fractional orders. The graphical simulations for all population compartments of the proposed model at $\vartheta = 0.75, 0.85, 0.95, 1$ are depicted in Figures 3(a–d), and 4(a–d).

This simulation has a greater degree of flexibility and can be adjusted to achieve distinct responses from the different compartments. The graphical observations from Figure 3(a–d), the susceptible population $S(z)$ is decreasing initially and after 10 weeks it increases.
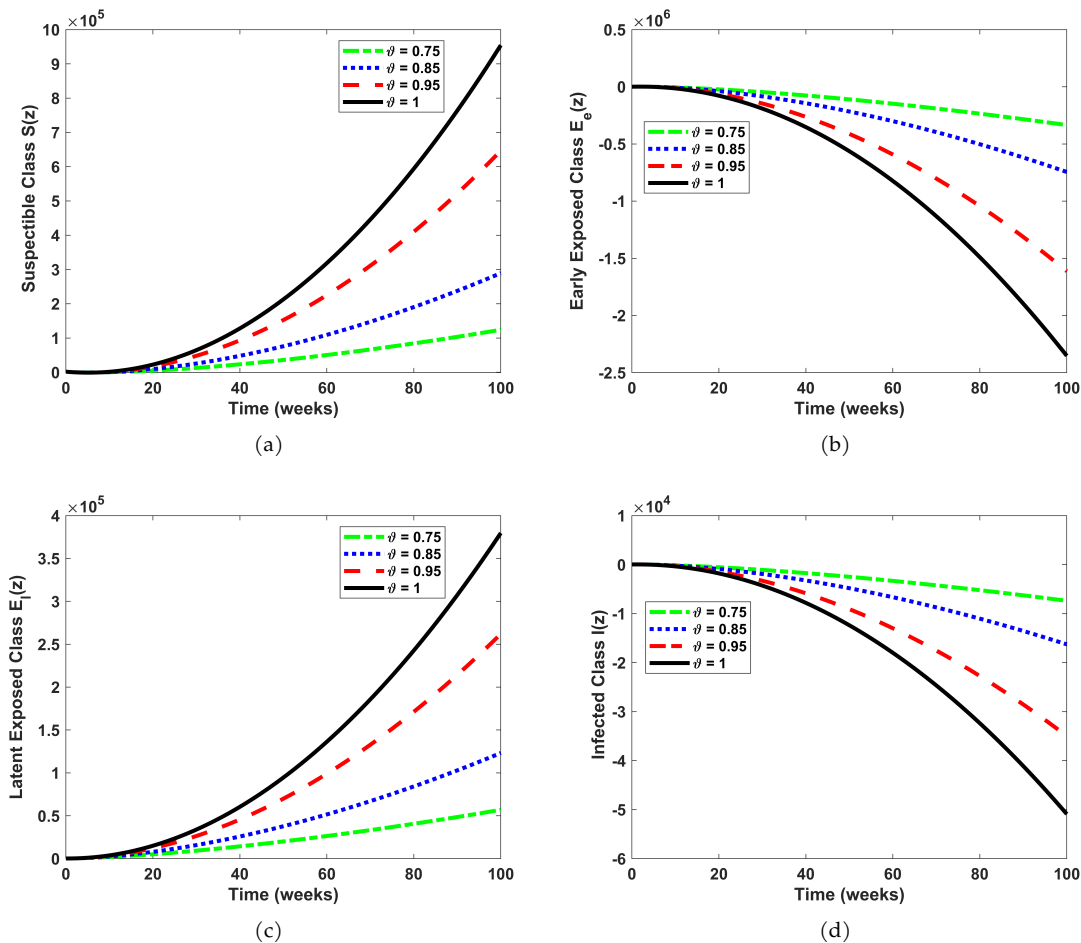
Figure 3: A graphic view of susceptible, early exposed, latent exposed and infected human population compartments on arbitrary orders ϑ.

The early exposed population $E_e(z)$ is increasing initially and after 2 weeks it decreases. The latent exposed population $E_l(z)$ is decreasing initially and after 3–4 days it increases. The infected population $I(z)$ is increasing initially and after one and half week it decreases. The treatment population $T(z)$ is increasing initially and after 10 weeks it decreases. The treatment interrupted population $G(z)$ is continuously increasing. Figure 4(c–d) illustrates, the low risk population $L_r(z)$ and recovered population $R(z)$ are increasing rapidly throughout the time duration. The steady–state solution at the fractional order derivative yields more consistent and effective results than the standard solution at $\vartheta = 1$. We observed from the graphical results, that the infection population decreases due to growth in low risk individuals, it means separation from infected individuals can cause to decrease the effects of disease. Figure 5 shows a graphical representation of the proposed Model (2) at $\vartheta = 1$ for $z \in [0, 40]$, which shows that the proposed model is stable and convergent.
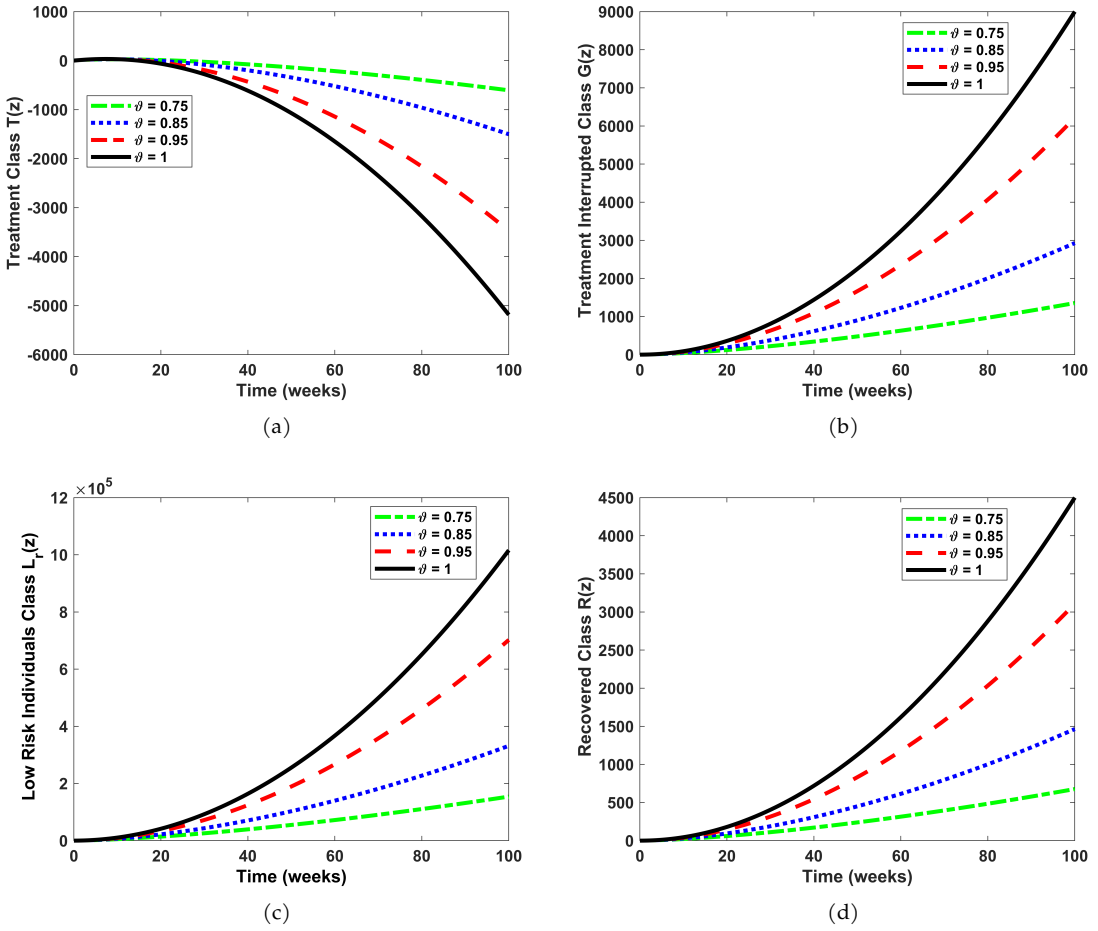
Figure 4: A graphic view of treatment, treatment interrupted, low risk and recovered human population compartments on arbitrary orders ϑ.
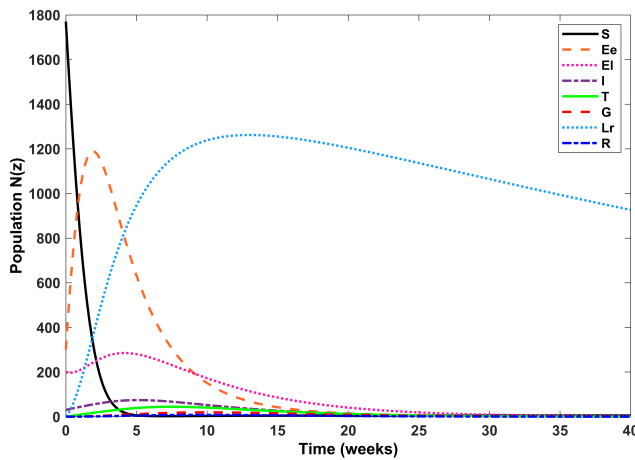

Figure 5: Graphic view of all compartments of the Model (2) for $z \in [0, 40]$.

7   Conclusions

In this article, we have investigated the transmission dynamics of TB infection using a mathematical model that incorporates the low risk individuals. The model was formulated in a non–classical derivative of Caputo differential equations of fractional order. Initially, we analyzed the TB model with the Caputo derivative, providing fundamental mathematical insights into the fractional model. Subsequently, we established the existence and uniqueness of solution of the model. We analyzed stability of the fractional–order TB model, stability analysis can help identify the critical values of parameters like the contact rate, treatment rate, and fractional order that determine the stability of disease–free and endemic equilibria. The biological feasibility of the stability order are crucial for developing reliable and accurate models in epidemiology and other biological applications. This information can guide public health interventions and control strategies. Furthermore, a sensitivity study was also performed to assess the relative impact of different parameters of the model on TB spread.

Our observations indicated that reducing the parameter σ value led to a decrease in the overall number of infected cases. Numerical simulations were conducted and graphically interpreted for arbitrarily chosen orders. Graphical representations demonstrated a notable dependence of results on the parameters values, exhibiting distinct outcomes for different values of ϑ. Notably, decreasing the parameters values significantly reduced the infectious TB population. Moreover, we noticed that the number of infected people goes down because there are more low–risk individuals, which means that staying away from infected people can help to reduce the effects of the disease. This comprehensive knowledge provides a unique perspective on TB dynamics, offering valuable insights for public health officials and policy makers to develop a more effecting disease control and prevention strategies. Moreover, researchers can explore how stable the fractional order TB disease model is by using different approaches. In future, we will study comparison analysis of the outcomes of our proposed model with homotopy perturbation method and fractional differential transform method.

Conflicts of Interest The authors declare no conflict of interest.

References

[1] O. Abdulaziz, I. Hashim & S. Momani (2008). Solving systems of fractional differential equations by homotopy-perturbation method. *Physics Letters A*, *372*(4), 451–459. https://doi.org/10.1016/j.physleta.2007.07.059.

[2] S. Ahmad, R. Ullah & D. Baleanu (2021). Mathematical analysis of tuberculosis control model using nonsingular kernel type Caputo derivative. *Advances in Difference Equations*, *2021*, Article ID: 26. https://doi.org/10.1186/s13662-020-03191-x.

[3] Q. M. Al-Mdallal (2023). Mathematical modeling and simulation of SEIR model for COVID-19 outbreak: A case study of Trivandrum. *Frontiers in Applied Mathematics and Statistics*, *9*, Article ID: 1124897. https://doi.org/10.3389/fams.2023.1124897.

[4] S. M. Al-Zahrani, F. E. I. Elsmih, K. S. Al-Zahrani & S. Saber (2022). A fractional order SITR model for forecasting of transmission of COVID–19: sensitivity statistical analysis. *Malaysian Journal of Mathematical Sciences*, *16*(3), 517–536. https://doi.org/10.47836/mjms.16.3.08.

[5] G. E. Ali, A. A. Asaad, S. K. Elagan, E. Mawaheb & M. S. AlDien (2017). Using Laplace transform method for obtaining the exact analytic solutions of some ordinary fractional differential equations. *Global Journal of Pure and Applied Mathematics*, *13*(9), 5021–5035.

[6] A. S. Alshomrani, M. Z. Ullah & D. Baleanu (2021). Caputo SIR model for COVID-19 under optimized fractional order. *Advances in Difference Equations*, *2021*(1), Article ID: 185. https://doi.org/10.1186/s13662-021-03345-5.

[7] S. Arshad, I. Siddique, F. Nawaz, A. Shaheen & H. Khurshid (2023). Dynamics of a fractional order mathematical model for COVID-19 epidemic transmission. *Physica A: Statistical Mechanics and its Applications*, *609*, Article ID: 128383. https://doi.org/10.1016/j.physa.2022.128383.

[8] A. Asres, D. Jerene & W. Deressa (2018). Delays to treatment initiation is associated with tuberculosis treatment outcomes among patients on directly observed treatment short course in Southwest Ethiopia: A follow-up study. *BMC pulmonary medicine*, *18*, Article ID: 64. https://doi.org/10.1186/s12890-018-0628-2.

[9] W. Atokolo, R. O. Aja, S. E. Aniaku, I. S. Onah & G. C. E. Mbah (2022). Approximate solution of the fractional order sterile insect technology model via the Laplace–Adomian Decomposition Method for the spread of Zika virus disease. *International Journal of Mathematics and Mathematical Sciences*, *2022*(1), Article ID: 2297630. https://doi.org/10.1155/2022/2297630.

[10] Z. Avazzadeh, H. Hassani, P. Agarwal, S. Mehrabi, M. J. Ebadi & M. S. Dahaghin (2023). An optimization method for studying fractional-order tuberculosis disease model via generalized Laguerre polynomials. *Soft Computing*, *27*(14), 9519–9531. https://doi.org/10.1007/s00500-023-08086-z.

[11] D. Baleanu, A. Jajarmi, S. S. Sajjadi & D. Mozyrska (2019). A new fractional model and optimal control of a tumor-immune surveillance with non-singular derivative operator. *Chaos: An Interdisciplinary Journal of Nonlinear Science*, *29*(8), Article ID: 083127. https://doi.org/10.1063/1.5096159.

[12] D. Baleanu, H. Mohammadi & S. Rezapour (2020). A mathematical theoretical study of a particular system of Caputo–Fabrizio fractional differential equations for the Rubella disease model. *Advances in Difference Equations*, *2020*, Article ID: 184. https://doi.org/10.1186/s13662-020-02614-z.

[13] D. Baleanu, P. Shekari, L. Torkzadeh, H. Ranjbar, A. Jajarmi & K. Nouri (2023). Stability analysis and system properties of Nipah virus transmission: A fractional calculus case study. *Chaos, Solitons & Fractals*, *166*, Article ID: 112990. https://doi.org/10.1016/j.chaos.2022.112990.

[14] C. P. Bhunu (2011). Mathematical analysis of a three-strain tuberculosis transmission model. *Applied Mathematical Modelling*, *35*(9), 4647–4660. https://doi.org/10.1016/j.apm.2011.03.037.

[15] O. Defterli, D. Baleanu, A. Jajarmi, S. S. Sajjadi, N. Alshaikh & J. H. Asad (2022). Fractional treatment: an accelerated mass–spring system. *Romanian Reports in Physics*, *74*, Article ID: 122.

[16] K. Diethelm (2010). *The Analysis of Fractional Differential Equations*. Lecture Notes in Mathematics. Springer, Berlin, Heidelberg. https://doi.org/10.1007/978-3-642-14574-2.

[17] M. Farman, A. Shehzad, A. Akgül, E. Hincal, D. Baleanu & S. M. El Din (2023). A fractal-fractional sex structured syphilis model with three stages of infection and loss of immunity with analysis and modeling. *Results in Physics*, *54*, 107098. https://doi.org/10.1016/j.rinp.2023.107098.

[18] W. Gao, P. Veeresha, D. Prakasha, H. M. Baskonus & G. Yel (2020). New approach for the model describing the deathly disease in pregnant women using Mittag-Leffler function. *Chaos, Solitons & Fractals*, *134*, Article ID: 109696. https://doi.org/10.1016/j.chaos.2020.109696.

[19] S. Georgiev (2023). Mathematical identification analysis of a fractional-order delayed model for tuberculosis. *Fractal and Fractional*, *7*(7), Article ID: 538. https://doi.org/10.3390/fractalfract7070538.

[20] K. Hattaf, M. Rachik, S. Saadi, Y. Tabit & N. Yousfi (2009). Optimal control of tuberculosis with exogenous reinfection. *Applied Mathematical Sciences*, *3*(5), 231–240.

[21] K. Hattaf (2023). A new class of generalized fractal and fractal-fractional derivatives with non-singular kernels. *Fractal and Fractional*, *7*(5), Article ID: 395. https://doi.org/10.3390/fractalfract7050395.

[22] K. Hattaf (2024). A new mixed fractional derivative with applications in computational biology. *Computation*, *12*(1), Article ID: 7. https://doi.org/10.3390/computation12010007.

[23] R. Hilfer (2000). *Applications of Fractional Calculus in Physics*. World Scientific, Singapore. https://doi.org/10.1142/3779.

[24] C. Ionescu, A. Lopes, D. Copot, J. A. T. Machado & J. H. T. Bates (2017). The role of fractional calculus in modeling biological phenomena: A review. *Communications in Nonlinear Science and Numerical Simulation*, *51*, 141–159. https://doi.org/10.1016/j.cnsns.2017.04.001.

[25] A. A. Kilbas, H. M. Srivastava & J. J. Trujillo (2006). *Theory and Applications of Fractional Differential Equations*. Elsevier, New York.

[26] S. Kim, E. Jung et al. (2018). Mathematical model and intervention strategies for mitigating tuberculosis in the Philippines. *Journal of Theoretical Biology*, *443*, 100–112. https://doi.org/10.1016/j.jtbi.2018.01.026.

[27] D. Kumar, J. Singh, M. Al Qurashi & D. Baleanu (2019). A new fractional SIRS-SI malaria disease model with application of vaccines, antimalarial drugs, and spraying. *Advances in Difference Equations*, *2019*(1), 1–19. https://doi.org/10.1186/s13662-019-2199-9.

[28] S. Kumar, R. P. Chauhan, S. Momani & S. Hadid (2021). A study of fractional TB model due to mycobacterium tuberculosis bacteria. *Chaos, Solitons & Fractals*, *153*(Part 2), 111452. https://doi.org/10.1016/j.chaos.2021.111452.

[29] J. Liu & T. Zhang (2011). Global stability for a tuberculosis model. *Mathematical and Computer Modelling*, *54*(1-2), 836–845. https://doi.org/10.1016/j.mcm.2011.03.033.

[30] L. Liu & Y. Wang (2014). A mathematical study of a TB model with treatment interruptions and two latent periods. *Computational and Mathematical Methods in Medicine*, *2014*(1), Article ID: 932186. https://doi.org/10.1155/2014/932186.

[31] K. Luo (2013). A novel self–adaptive harmony search algorithm. *Journal of Applied Mathematics*, *2013*(1), Article ID: 653749. https://doi.org/10.1155/2013/653749.

[32] R. Magin (2004). Fractional calculus in bioengineering, part 1. *Critical Reviews in Biomedical Engineering*, *32*(1), 1–36. https://doi.org/10.1615/CritRevBiomedEng.v32.i1.

[33] A. Mohandoss, G. Chandrasekar, M. Z. Meetei & A. H. Msmali (2024). Fractional order mathematical modelling of HFMD transmission via Caputo derivative. *Axioms*, *13*(4), Article ID: 213. https://doi.org/10.3390/axioms13040213.

[34] M. Nicas, W. W. Nazaroff & A. Hubbard (2005). Toward understanding the risk of secondary airborne infection: Emission of respirable pathogens. *Journal of Occupational and Environmental Hygiene*, *2*(3), 143–154. https://doi.org/10.1080/15459620590918466.

[35] K. S. Nisar & M. Farman (2024). Analysis of a mathematical model with hybrid fractional derivatives under different kernel for hearing loss due to mumps virus. *International Journal of Modelling and Simulation*, *2024*(2), 1–27. https://doi.org/10.1080/02286203.2024.2322361.

[36] K. S. Nisar, M. Farman, A. Zehra & E. Hincal (2024). Numerical and analytical study of fractional order tumor model through modeling with treatment of chemotherapy. *International Journal of Modelling and Simulation*, *2024*, 1–14. https://doi.org/10.1080/02286203.2024.2327659.

[37] M. O. Olayiwola, A. I. Alaje, A. Y. Olarewaju & K. A. Adedokun (2023). A Caputo fractional order epidemic model for evaluating the effectiveness of high-risk quarantine and vaccination strategies on the spread of COVID-19. *Healthcare Analytics*, *3*, Article ID: 100179. https://doi.org/10.1016/j.health.2023.100179.

[38] K. M. Owolabi & E. Pindza (2022). A nonlinear epidemic model for tuberculosis with Caputo operator and fixed point theory. *Healthcare Analytics*, *2*, Article ID: 100111. https://doi.org/10.1016/j.health.2022.100111.

[39] F. Özköse (2023). Fractional mathematical modelling of the spread of rotavirus disease. *Erciyes Üniversitesi Fen Bilimleri Enstitüsü Fen Bilimleri Dergisi*, *39*(2), 253–270.

[40] P. Phaochoo, C. Wisseksakwichai, N. Thongpool, S. Chankong & K. Promluang (2023). Application of fractional derivative for the study of chemical reaction. *International Journal of Intelligent Networks*, *13*, Article ID: 2245.

[41] S. Rashid, Y. G. Sánchez, J. Singh & K. M. Abualnaja (2022). Novel analysis of nonlinear dynamics of a fractional model for tuberculosis disease via the generalized Caputo fractional derivative operator (case study of Nigeria). *American Institute of Mathematical Sciences Mathematics*, *7*(6), 10096–10121. https://doi.org/10.3934/math.2022562.

[42] W. Shatanawi, M. S. Abdo, M. A. Abdulwasaa, K. Shah, S. K. Panchal, S. V. Kawale & K. P. Ghadle (2021). A fractional dynamics of tuberculosis (TB) model in the frame of generalized Atangana–Baleanu derivative. *Results in Physics*, *29*, Article ID: 104739. https://doi.org/10.1016/j.rinp.2021.104739.

[43] M. Sinan, H. Ahmad, Z. Ahmad, J. Baili, S. Murtaza, M. A. Aiyashi & T. Botmart (2022). Fractional mathematical modeling of Malaria disease with treatment & insecticides. *Results in Physics*, *34*, Article ID: 105220. https://doi.org/10.1016/j.rinp.2022.105220.

[44] A. Tassaddiq, S. Qureshi, A. Soomro, O. A. Arqub & M. Senol (2024). Comparative analysis of classical and Caputo models for COVID-19 spread: Vaccination and stability assessment. *Fixed Point Theory and Algorithms for Sciences and Engineering*, *2024*(1), Article ID: 2. https://doi.org/10.1186/s13663-024-00760-7.

[45] G. T. Tilahun, O. D. Makinde & D. Malonza (2017). Modelling and optimal control of typhoid fever disease with cost-effective strategies. *Computational and Mathematical Methods in Medicine*, *2017*(1), Article ID: 2324518. https://doi.org/10.1155/2017/2324518.

[46] M. Z. Ullah, A. K. Alzahrani & D. Baleanu (2019). An efficient numerical technique for a new fractional tuberculosis model with nonsingular derivative operator. *Journal of Taibah University for Science*, 13(1), 1147–1157. https://doi.org/10.1080/16583655.2019.1688543.

[47] H. Waaler, A. Geser & S. Andersen (1962). The use of mathematical models in the study of the epidemiology of tuberculosis. *American Journal of Public Health and the Nations Health*, 52(6), 1002–1013. https://doi.org/10.2105/ajph.52.6.1002.

[48] WHO. Global tuberculosis report 2022. https://www.who.int/news-room/fact-sheets/detail/tuberculosis.

[49] S. Widatalla (2012). A comparative study on the stability of Laplace-Adomian algorithm and numerical methods in generalized pantograph equations. *International Scholarly Research Notices*, 2012(1), Article ID: 704184. https://doi.org/10.5402/2012/704184.

[50] J. Zhang, Y. Li & X. Zhang (2015). Mathematical modeling of tuberculosis data of China. *Journal of Theoretical Biology*, 365, 159–163. https://doi.org/10.1016/j.jtbi.2014.10.019.

[51] X. H. Zhang, A. Ali, M. A. Khan, M. Y. Alshahrani, T. Muhammad & S. Islam (2021). Mathematical analysis of the TB model with treatment via Caputo-type fractional derivative. *Discrete Dynamics in Nature and Society*, 2021(1), Article ID: 9512371. https://doi.org/10.1155/2021/9512371.